ISPRS Journal of Photogrammetry and Remote Sensing 65 (2010) 42–59

Contents lists available at ScienceDirect

ISPRS Journal of Photogrammetry and Remote Sensing

journal homepage: www.elsevier.com/locate/isprsjprs

Irrigated areas of India derived using MODIS 500 m time series for the years 2001–2003

V. Dheeravath [a], P.S. Thenkabail [b,*], G. Chandrakantha [c], P. Noojipady [d], G.P.O. Reddy [e], C.M. Biradar [f], M.K. Gumma [g], M. Velpuri [h]

[a] United Nations Joint Logistic Center-WFP, Juba, South Sudan, Sudan
[b] Southwest Geographic Science Center, US Geological Survey, Flagstaff, AZ, USA
[c] Department of Applied Geology, Kuvempu University, Karnataka, India
[d] Department of Geography, University of Maryland, USA
[e] National Bureau of Soil Survey and Land Use Planning, Nagpur, India
[f] University of Oklahoma, 101 David L. Boren Blvd, Norman, OK 73019, USA
[g] International Water Management Institute, Hyderabad, India
[h] Geographic Information Science Center of Excellence, South Dakota State University, USA

ARTICLE INFO

Article history:
Received 12 September 2008
Received in revised form
3 August 2009
Accepted 21 August 2009
Available online 22 September 2009

Keywords:
Agriculture
Land use
Crop
Hyperspectral
Vegetation

ABSTRACT

The overarching goal of this research was to develop methods and protocols for mapping irrigated areas using a Moderate Resolution Imaging Spectroradiometer (MODIS) 500 m time series, to generate irrigated area statistics, and to compare these with ground- and census-based statistics. The primary mega-file data-cube (MFDC), comparable to a hyper-spectral data cube, used in this study consisted of 952 bands of data in a single file that were derived from MODIS 500 m, 7-band reflectance data acquired every 8-days during 2001–2003. The methods consisted of (a) segmenting the 952-band MFDC based not only on elevation-precipitation-temperature zones but on major and minor irrigated command area boundaries obtained from India's Central Board of Irrigation and Power (CBIP), (b) developing a large ideal spectral data bank (ISDB) of irrigated areas for India, (c) adopting quantitative spectral matching techniques (SMTs) such as the spectral correlation similarity (SCS) R^2-value, (d) establishing a comprehensive set of protocols for class identification and labeling, and (e) comparing the results with the National Census data of India and field-plot data gathered during this project for determining accuracies, uncertainties and errors. The study produced irrigated area maps and statistics of India at the national and the subnational (e.g., state, district) levels based on MODIS data from 2001–2003. The Total Area Available for Irrigation (TAAI) and Annualized Irrigated Areas (AIAs) were 113 and 147 million hectares (MHa), respectively. The TAAI does not consider the intensity of irrigation, and its nearest equivalent is the net irrigated areas in the Indian National Statistics. The AIA considers intensity of irrigation and is the equivalent of "irrigated potential utilized (IPU)" reported by India's Ministry of Water Resources (MoWR). The field-plot data collected during this project showed that the accuracy of TAAI classes was 88% with a 12% error of omission and 32% of error of commission. Comparisons between the AIA and IPU produced an R^2-value of 0.84. However, AIA was consistently higher than IPU. The causes for differences were both in traditional approaches and remote sensing. The causes of uncertainties unique to traditional approaches were (a) inadequate accounting of minor irrigation (groundwater, small reservoirs and tanks), (b) unwillingness to share irrigated area statistics by the individual Indian states because of their stakes, (c) absence of comprehensive statistical analyses of reported data, and (d) subjectivity involved in observation-based data collection process. The causes of uncertainties unique to remote sensing approaches were (a) irrigated area fraction estimate and related sub-pixel area computations and (b) resolution of the imagery. The causes of uncertainties common in both traditional and remote sensing approaches were definitions and methodological issues.

* Corresponding author. Tel.: +1 928 556 7221; fax: +1 928 556 7112.
E-mail addresses: vdheeravath@gmail.com (V. Dheeravath), thenkabail@gmail.com, pthenkabail@usgs.gov (P.S. Thenkabail).

0924-2716/$ – see front matter
doi:10.1016/j.isprsjprs.2009.08.004

Acronyms and abbreviations

2d-FS	2-Dimensional Feature Space
AIA	Annualized Irrigated Area
AOC	Area of Continuous Cropping in a Year
AVHRR	Advanced Very High Resolution Radiometer
CBIP	Central Board of Irrigation and Power
CC	Continuous Crop
CCA	Cultivable Command Area
CRU	Climatic Research Unit
DCP	Degree Confluence Project
ERDAS	Earth Resources Digital Analysis System
FAO	Food and Agriculture Organization of the United Nations
FPA	Full Pixel Area
GIS	Geographic Information System
GIAM	Global Irrigated Area Map
GE VHRI	Google Earth Very High Resolution Imagery
GSFC	Goddard Space Flight Center
IAF	Irrigated Area Fraction
IPU	Irrigation Potential Utilized
ISDB	Ideal Spectral Data Bank
IWMI	International Water Management Institute
IWMI-DSP	International Water Management Institute Data Storehouse Pathway
IWMI-GIAM	International Water Management Institute Global Irrigated Area Mapping
LULC	Land Use/Land Cover
MHa	Million Hectares
MODIS	Moderate Resolution Imaging Spectroradiometer
MoWR	Ministry of Water Resources
MVC	Maximum Value Composite
NASA	National Aeronautics and Space Administration
NDVI	Normalized Difference Vegetation Index
PWD	Public Works Department
SCS	Spectral Correlation Similarity
SOCLASS	Statistical Clustering Algorithm in ERDAS
SRTM	Shuttle Radar Topography Mission
SSV	Spectral Similarity Value
TAAI	Total Area Available for Irrigation.
UF	University of Frankfruit

1. Introduction, background and rationale

Irrigation consumes nearly 80% of all water used by humans (Döll and Siebert, 2002). However, there is great uncertainty in the actual area irrigated and the spatial location of irrigated areas. This in turn leads to uncertainties in estimates of actual water use by irrigation. In most parts of the world, irrigated areas are reported based on census data. In India, for example, traditional local-level revenue department officials report irrigation statistics at the village level which is then aggregated to higher levels, such as *tehsil* (a lower administrative unit like a county), district, state, and national levels (Reddy et al., 2006). Added to the fact that the quality of the compiled data is often called into question (Biggs et al., 2006; Droogers, 2002), such a process is tedious, time-consuming, inconsistent, and resource-intensive. Remote sensing offers a potential solution, and some early remote-sensing applications involved mapping irrigated croplands (Huston and Titus, 1975; Draeger, 1976; Wall, 1979; Thiruvengadachari, 1981) to create inventories of areas irrigated from different irrigation sources such as surface water, groundwater and irrigation tanks (Thiruvengadachari, 1983; Thiruvengadachari and Sakthivadivel, 1997). Such mapping enables the assessment of crop stress, discrimination of crop types, and monitoring temporal changes in irrigated areas (Azzali and Menenti, 1989; Rao and Mohankumar, 1994; Thiruvengadachari and Sakthivadivel, 1997). The advanced remote-sensing applications involve different techniques and methods using the hyperspectral and time-series multispectral data to map Land Use/Land Cover (LULC), crop phenology and cropping systems (Thenkabail et al., 2009a,b; Galford et al., 2008; Wardlow et al., 2007; Wardlow and Egbert, 2008; Sakamoto et al., 2005, 2006; Thenkabail et al., 2005).

Irrigated areas have rarely been mapped over large areas such as a subcontinent, a continent, and the globe. Exceptions are the recent work by the International Water Management Institute (IWMI) as described by Thenkabail et al. (2009a,b, 2006) and Biradar et al. (2009), and the product of the Food and the Agricultural Organization of the United Nations and the University of Frankfurt (FAO/UF) as described by Siebert et al. (2002, 2005, 2006), which is a compilation of the national statistics into a spatial map and having a minimum resolution of 10 km. The IWMI study is based on multiple satellite-sensors-based time series of remote sensing and secondary data and is reported at a minimum 1 km resolution. Sakamoto et al. (2005, 2006) used MODIS time series to detect spatiotemporal crop phenology and cropping systems at the river basin and regional scale. In other LULC maps (Wardlow et al., 2007; Wardlow and Egbert, 2008; Bartholome and Belward, 2005; Lobell and Asner, 2004; Agarwal et al., 2003) irrigated areas are just one of the many classes, not the focus of the study, and are often a mix-up of rain-fed and irrigated areas.

Historically, fine spatial resolution irrigated area mapping using remote sensing has been limited to small areas such as river basins (Biggs et al., 2006; Thenkabail et al., 2005; Thiruvengadachari and Sakthivadivel, 1997) or the regional level (Wardlow and Egbert, 2008; Xiao et al., 2006). The improvements in spatial, spectral and temporal resolution and advances in calibration and normalization of modern satellite sensor data allow irrigated area mapping over larger areal extents. In the case of MODIS (Justice et al., 2003), 500 m data are available frequently (every 8-days) and they have global coverage, undergo ongoing validation, are free of charge to the user, and are easily accessed via the Internet. Further, this frequent availability enables monthly composites of the data that remove an overwhelming proportion of cloud cover, enables the derivation of crop calendars and helps in the study of irrigated and nonirrigated area dynamics (Biggs et al., 2006). The MODIS time series are powerful for agricultural intensification of crops from season to season to mark the changes of cropping calendars (Galford et al., 2008).

Taking advantage of the advances in remotely sensed data, the overarching goal of this research was to develop methods and protocols for mapping irrigated areas of India using a MODIS time series (500 m resolution, from 2001 to 2003). India was selected as the study area for several reasons. First, the country is the first (Siebert et al., 2006) or the second (Thenkabail et al., 2009a) most irrigated country in the world along with China. Second, the field-plot data and national statistical data on irrigated areas were available for the country for comparison with satellite-sensor-derived data. Third, the population of 1.1 billion with a rapidly growing economy makes India an interesting country for a study on irrigated areas, their water use, food production, and food security issues.

The specific objectives of the study were to (a) map irrigated areas of India using MODIS every 8-day, 7-band, time series for 2001–2003, (b) provide irrigated area statistics at the state and the district level, (c) compare MODIS-based irrigated area statistics with the national census reported and field-plot gathered data, (d) discuss the Sub-Pixel Area (SPA) calculation methods and highlight their importance in area calculations, (e) determine accuracies, uncertainties and errors in reporting irrigated areas using MODIS, and (f) provide a comprehensive discussion on causes of uncertainties and errors in computing and reporting irrigated areas.

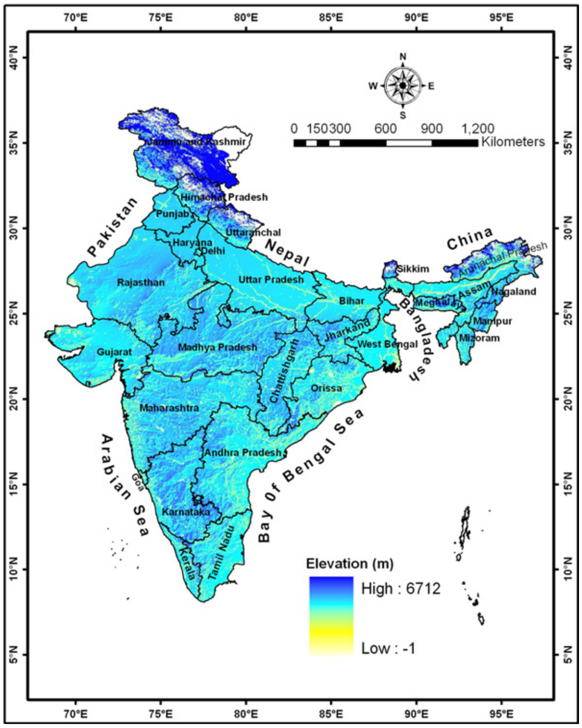

Fig. 1. The study area shows Indian administrative state and district boundaries overlain on Shuttle Radar Topography Mission (SRTM) 90 m data.

2. Study area

The total available arable land of India (Fig. 1) was reported as 56% (of the total geographic area of 330 MHa) in 2004 while permanent crops covered 1%, permanent pastures accounted for 4%, forest and woodlands covered 23% and other LULC 16% (Lal, 2004). Irrigation projects in India which have a cultivable command area (CCA) more than 10,000 ha are termed as major projects, those with a CCA between 2000 and 10,000 ha are termed as medium projects, and those with a CCA less than 2000 ha are known as minor projects.

3. Methodology

The methodology begins with definitions used in mapping irrigated areas, followed by descriptions of the datasets (MODIS and field-plot), data processing and the creation of an ideal spectral data bank, class spectra generation, and a class identification and labeling process that starts with spectral matching techniques.

3.1. Definition used in mapping irrigated areas

The MODIS-derived irrigated areas were calculated using SPA calculation methods, which are described in detail by Thenkabail et al. (2007b). The full pixel areas (FPAs) of the classes were multiplied by the irrigated area fractions (IAFs; Thenkabail et al., 2007b) to obtain SPAs. The irrigated areas were calculated with and without intensity as described in the subsequent sections.

3.1.1. Total Area Available for Irrigation (TAAI): Areas without considering the intensity of irrigation

The TAAI is the area irrigated at any given point of time, plus the area left fallow (but equipped for irrigation) at the same point of time. The TAAI does not consider intensity (areas from different seasons). This would mean that if we map irrigated areas using data of, say, cropping season 1 (e.g., June to October), then the areas irrigated during cropping season 1 will be (a) area actually irrigated during season 1, plus (b) area left fallow in season 1. The sum of (a) and (b) is TAAI. Typically, some areas have only one crop a year, others two, and some areas have continuous year-round (e.g., sugarcane) crops. However, the overall TAAI remains constant across the seasons. What changes from season to season within the TAAI will be the ratio of area irrigated to area left fallow. Typically, in the main cropping season (*kharif*, or June to October) in India, the actual area irrigated is the maximum with the area left fallow being the minimum. This trend changes in the *rabi* season (November to February) when fallow areas increase and cropped areas decrease. However, irrespective of the season TAAI remains constant with variation in the proportion of irrigated areas to fallow areas. The nearest equivalent of TAAI in the Food and Agricultural Organization of the United Nations and the University of Frankfurt (FAO/UF; Siebert et al., 2006) are "areas equipped for irrigation" (but not necessarily irrigated) (Siebert et al., 2006). The equivalent of TAAI in the national statistics is Net Irrigated Areas.

3.1.2. Annualized Irrigated Areas (AIA): Areas considering the intensity of irrigation

The annualized irrigated areas (AIAs) are defined as the sum of the irrigated areas during a different crop-growing seasons (e.g., season 1, 2, and continuous year-round). Thus, AIA considers the intensity of irrigation. For each class, a cropping calendar is derived from time-series NDVI of the class to determine seasonality (or whether the area has single, double, or triple cropping). There is no nearest equivalent of AIA in FAO/UF-derived statistics. In the Indian national statistics, the nearest equivalent of annually averaged irrigated areas is Irrigation Potential Utilized (IPU) as defined in India's Ministry of Water Resources (MoWR, 2005) and also, at times, referred to as Gross Irrigated Areas (GIAs).

3.2. Data sets used in the study

3.2.1. MODIS data

The MODIS/Terra Surface Reflectance 8-day composite 500 m product (MOD09A1) utilizes the best observations during an 8-day period, as determined by overall pixel quality and observational coverage (Vermote et al., 2002; Xiao et al., 2006). The data were downloaded from the National Aeronautics and Space Administration Goddard Space Flight Center (NASA GSFC) for the years from 2001 to 2003. The study area was covered by 11 MODIS reflectance tiles. The mosaiced images were arranged in a continuous time series and compiled into a single MFDC consisting of 952 bands (a total of 136 images, each of 7 bands, over the same area during 2001–2003). The 952-band MFDC was used to (a) determine classes based on time-series characteristics rather than on a single date and/or a few dates; (b) obtain time-series characteristics of every pixel at the click of a mouse; and (c) facilitate the simplicity of handling a single file in data analysis. The MFDC was corrected for cloud cover and haze cover using approaches described in Thenkabail et al. (2005). The key steps involved were:

- Blue band minimum reflectivity threshold for cloud cover/haze removal or reduction.
- Visible band minimum reflectivity threshold for cloud cover/haze removal or reduction.
- Normalization of temporal variability.

Vegetation indices were also used to study and resolve classes. Indices reduce data volume and were considered the best approach to (a) remove clouds, (b) reduce data volume, and (c) enrich data to provide normalized information.

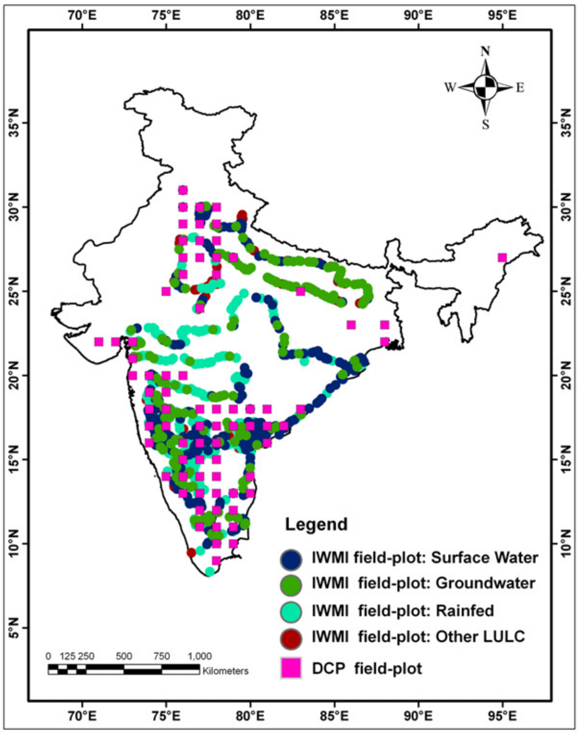

Fig. 2. The location of the field-plot data points collected during the project. Of the total 1041 field-plot data points, 951 were gathered during this project and the remaining 90 derived from degree confluence project (DCP).

3.2.2. Field-plot data

The project team gathered extensive data from field-plots as well as from other sources (Fig. 2). The data were gathered from irrigated areas, rain-fed cropland areas, and other LULC locations. Altogether 1089 field-plot points were gathered in different campaigns, by the same group of individuals following a consistent design. Sample site locations were chosen based on a stratified random sampling, stratified by the road network and randomized by stopping at different land cover types along the road. Depending on the road conditions and land cover types, data were collected from different locations at an interval of 5–10 km under good road conditions and at a distance of 3–5 km under poor road conditions.

At each location, data collected consisted of (a) coordinates using Global Positioning System, (b) watering method (i.e., irrigated, rain-fed, supplemental), (c) irrigation type (i.e., major and medium irrigation from surface water, minor irrigation from groundwater, small reservoirs, and tanks); (d) crop types, (e) cropping pattern (or crop combinations), (f) cropping calendar, (g) scale of irrigation (i.e., large and small scale), (h) land cover categories (i.e., trees, shrubs, grasses, farmlands) and (i) land use types (i.e., irrigated, rain-fed or LULC). Each location had 2–4 digital photos. Indian agriculture can be categorized into two distinct seasons, kharif (June to October) and rabi (November to February). Irrigated agriculture exists in both seasons as well as for certain areas of year-round crops. Field-plot data were collected to cover both seasons.

The second form of field-plot data was derived from the degree confluence project (DCP). The DCP data were contributed by a network of volunteers who gathered data from precise geographic locations for every one-degree latitude and longitude and recorded land use (through description) and made available several digital photos per location (Thenkabail et al., 2009b). We converted these data into GIS formats (Fig. 2).

Additional field-plot data such as canals, reservoirs, agricultural farms and field canals were derived from the Google Earth Very High Resolution Imagery (GE VHRI). All the above data along with the image interpretation techniques and ancillary data were used in the identification and labeling of classes.

3.3. Data processing to generate and identify irrigated and nonirrigated classes

Data processing consisted of (a) the creation of an MFDC, (b) image segmentation of MFDC, based on elevation, precipitation, temperature and irrigation maps from national sources, (c) producing an ISDB, (d) generating class spectra through a classification process, (e) quantitatively matching class spectra with ISDB through SMTs, (f) determining methods for resolving mixed classes, and (g) developing standardized class identification and labeling protocols. In Fig. 3 an overview of the methodology is provided along with initial steps for data synthesis. We used MODIS 500 m, 7 bands, every 8-day surface reflectance product (MOD09A1) in this study. This product is not corrected for view geometry and surface anisotropy, but this does not have any significant adverse effect on the mapping of irrigated areas (see Xiao et al., 2006; Thenkabail et al., 2005). Others (e.g., Ozdogan and Gutman, 2008) have used Nadir Bidirectional Reflectance Distribution Function (BRDF)-Adjusted Reflectance (NBAR) data (MOD34B4) to map irrigated areas of the USA. NBAR data are corrected for view- and illumination-angle effects. In contrast, Brown et al. (2009) produced irrigated areas of the USA using surface reflectance data with equally good results as those of Ozdogan and Gutman (2008). Studies by Xiao et al. (2006); Thenkabail et al. (2005) and Brown et al. (2009) clearly demonstrate the use of surface reflectance products in irrigated area mapping.

3.3.1. Segmentation based on precipitation, temperature and elevation

The study area was divided into various climate and elevation zones using: (a) SRTM elevation, (b) AVHRR "skin" temperature for 1981–2000, and (c) CRU precipitation for 1961–2000. This led to six unique zones (Fig. 4(a)). We segmented the MFDC based on these zones, resulting in each of these six zones having 952 bands of data. An additional 7th zone was based on the irrigated command area boundaries (Fig. 4(b)) that shows the major and medium irrigated areas from surface water reservoirs according to the map produced by CBIP (1994). This is followed by classification and class identification for every zone separately using methods and procedures described in Section 3.3.2 through 3.5.2.

3.3.2. Creation of an ISDB for the irrigated areas of India

The precise field-plot knowledge enabled the development of an ideal (or target) spectral data bank for various irrigated areas of India (e.g., Fig. 5). The approach adopted involved selecting classes of similar irrigation patterns spread across the study area and characterizing their ideal spectral signatures such as "irrigated, surface water, rice, single crop (Fig. 5)". The points were then grouped based on similarity. This leads to, for example, the development of an ISDB such as "irrigated, surface water, rice, single crop" from 13 samples in zone 3 (Fig. 6(a)). The ISDBs of Fig. 6 were illustrated taking zone 3 and zone 5 (see Fig. 4(a) for zones) (a) irrigated rice (Fig. 6(a), (b)) irrigated cotton vs. sugarcane (Fig. 6(b), (c)) irrigated rice vs. rain-fed rice (Fig. 6(c) and (d)) irrigated vs. rain-fed vs. other LULC (Fig. 6(d)). The ISDBs may or may not be similar in different zones. For example, ISDBs were nearly similar in zone 3 versus zone 5 for: (a) "irrigated, surface water, rice, double crop" (Fig. 6(a) and (b)) "irrigated, corn" (Fig. 6(d)). However, they were distinctly different in magnitude in "irrigated, rice" (Fig. 6(c)). The irrigated areas were also differentiated by source of irrigation (surface water vs. groundwater; Fig. 6(a), (b)). Often, the field-plot data have shown that the conditions in the field depict crop dominance (one crop or two dominating the area with a number of other crops occupying smaller fractions of the area) rather than the dominance of any one mono or single crop. In such situations, ideal spectral signatures for crop dominance (rice dominance, cotton dominance) in irrigated and nonirrigated settings were also developed.

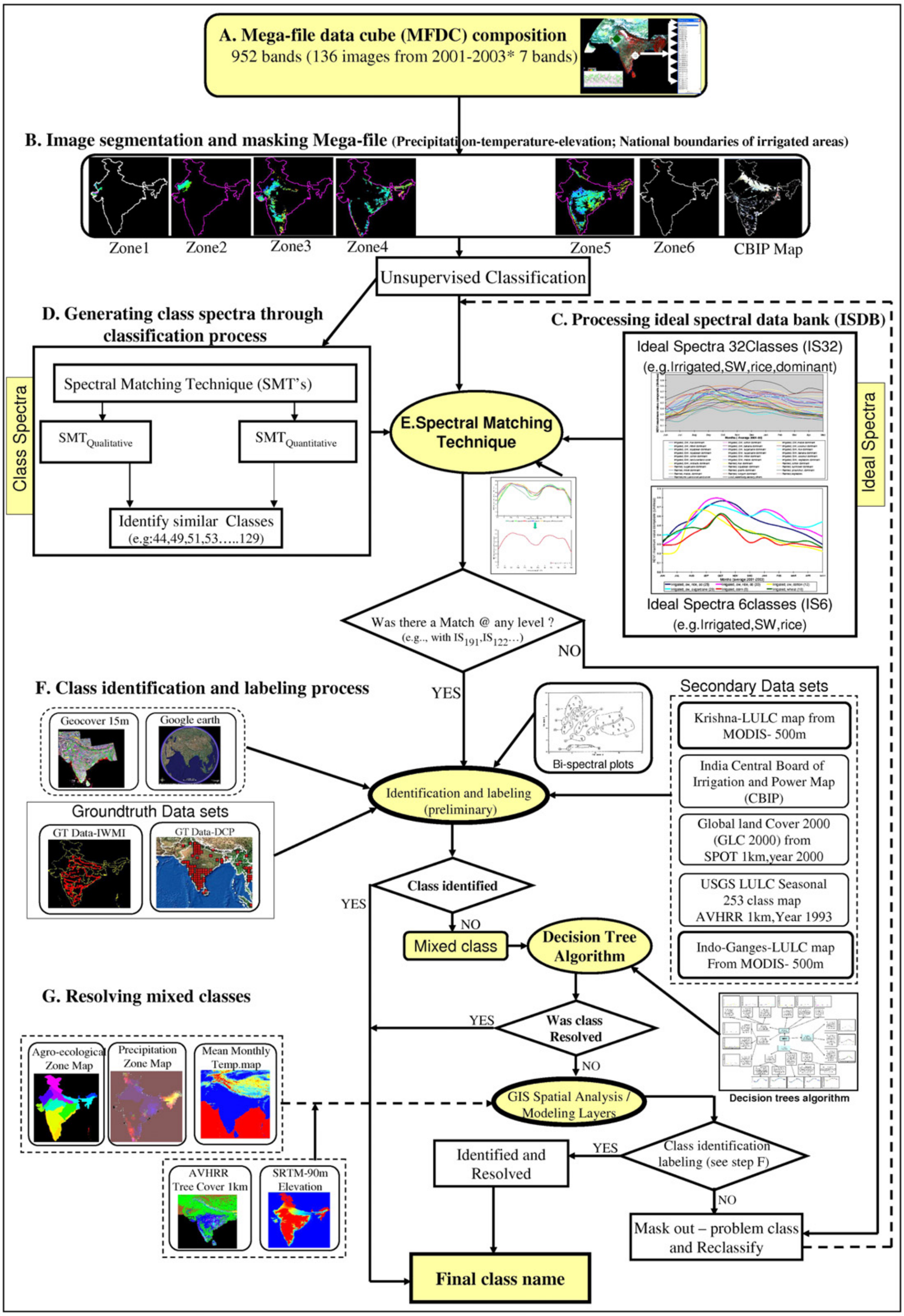

Fig. 3. The methodology for mapping irrigated areas using MODIS 500 m 7-band time-series surface reflectance product.

3.4. *Class spectra generation for irrigated areas of India*

The class spectra were generated using unsupervised ISOCLASS *k*-means classification (Tou and Gonzalez, 1975; Lieca, 2007) on the MODIS 500 m MFDC consisting of 952 bands for each of the seven zones (six zones in Fig. 4(a) and a single zone in Fig. 4(b)). Different classification methods (Lu and Weng, 2007) have their own merits. The ISOCLASS clustering has many advantages: (a) highly successful in finding spectral clusters in data, (b) interactive, (c) algorithm readily available and widely tested, (d) not biased to the top or the bottom of data, and (e) fastest-known method. The MFDCs of each of the segments were classified into 250 classes, and their time-series NDVI class spectra generated.

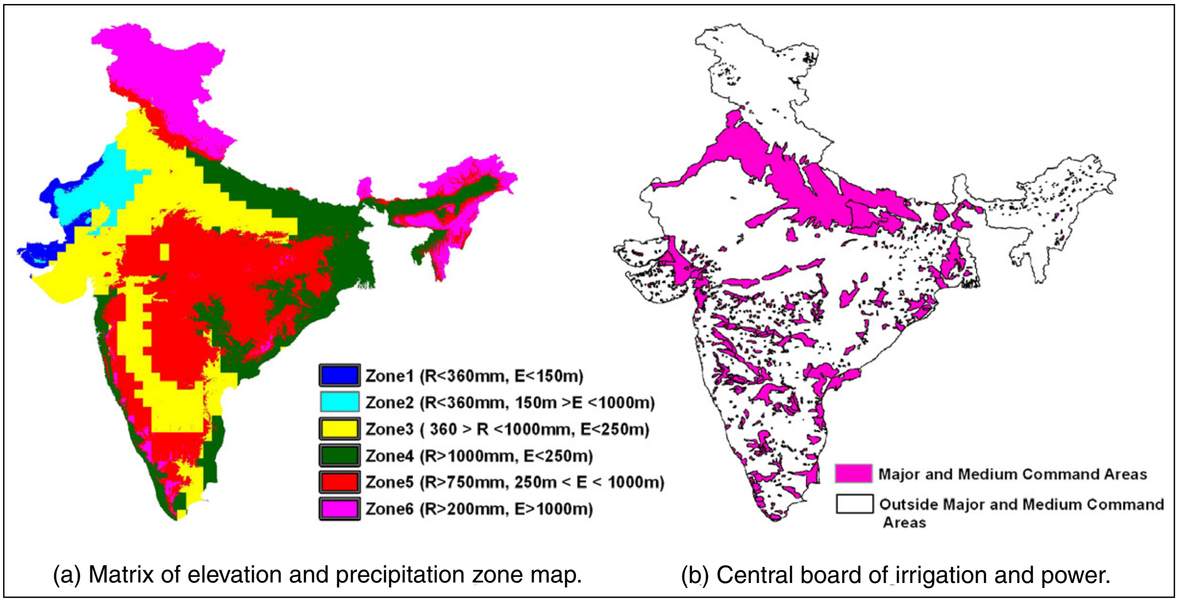

Fig. 4. The elevation-precipitation-temperature zones (left) and major irrigated area boundaries as per India's Central Board of Irrigation and Power (CBIP) (right) used to segment mega-file data cube (MFDC).

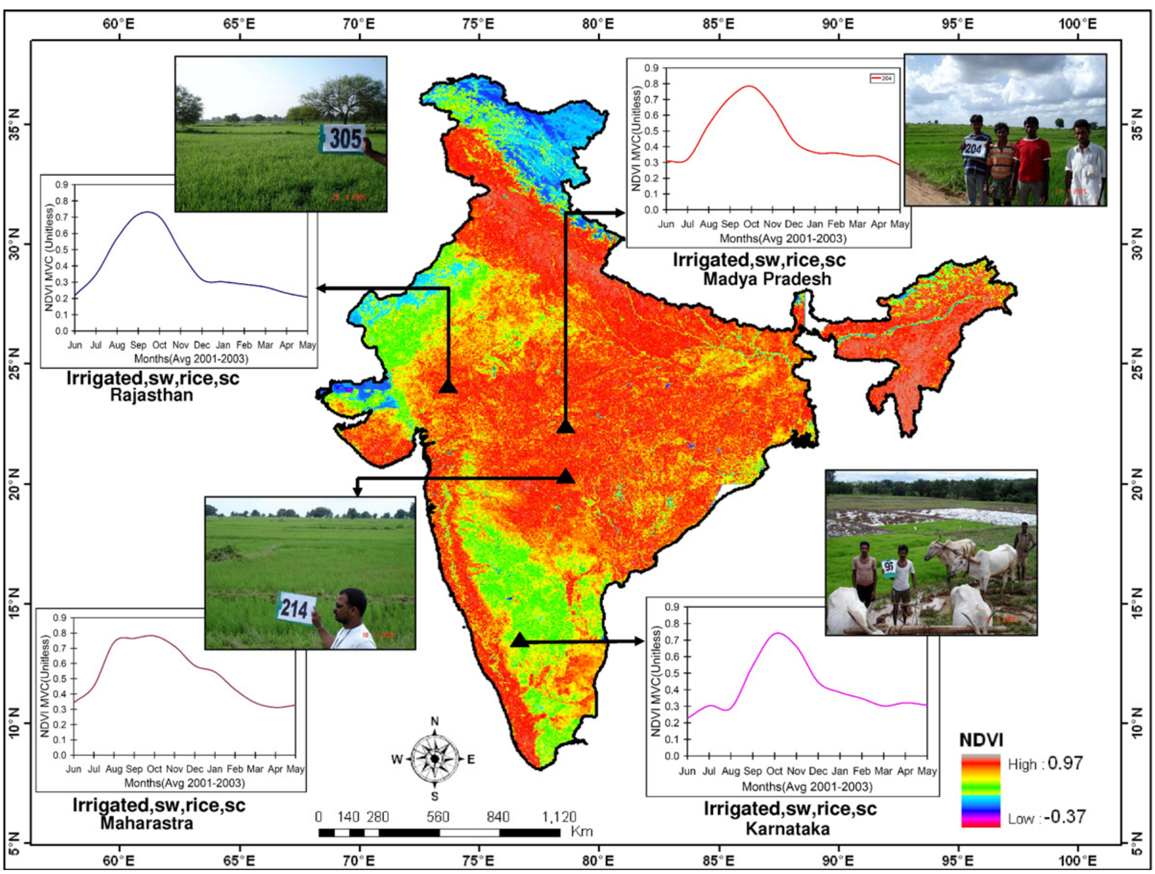

Fig. 5. Building ideal spectral data bank as illustrated for "irrigated-surface water-rice-single crop" using MODIS 500 m monthly NDVI MVC for the years 2001–2003 (note: the illustrations are shown for a few locations only).

3.5. Class identification and labeling process: Irrigated and nonirrigated classes

3.5.1. SMTs: Matching class spectra with ideal spectra

The class spectra were matched with ideal spectra using SMTs, which are traditionally developed for hyper-spectral data analysis of minerals (Homayouni and Roux, 2004) and adopted for irrigated area mapping using remotely sensed time series (Thenkabail et al., 2007b). In Fig. 7, classes 26, 28, 30 and 43 have very similar NDVI signatures that were subsequently grouped using the spectral correlation similarity R^2 values (SCS R^2) and the spectral similarity values according to Thenkabail et al. (2007a). The group of classes

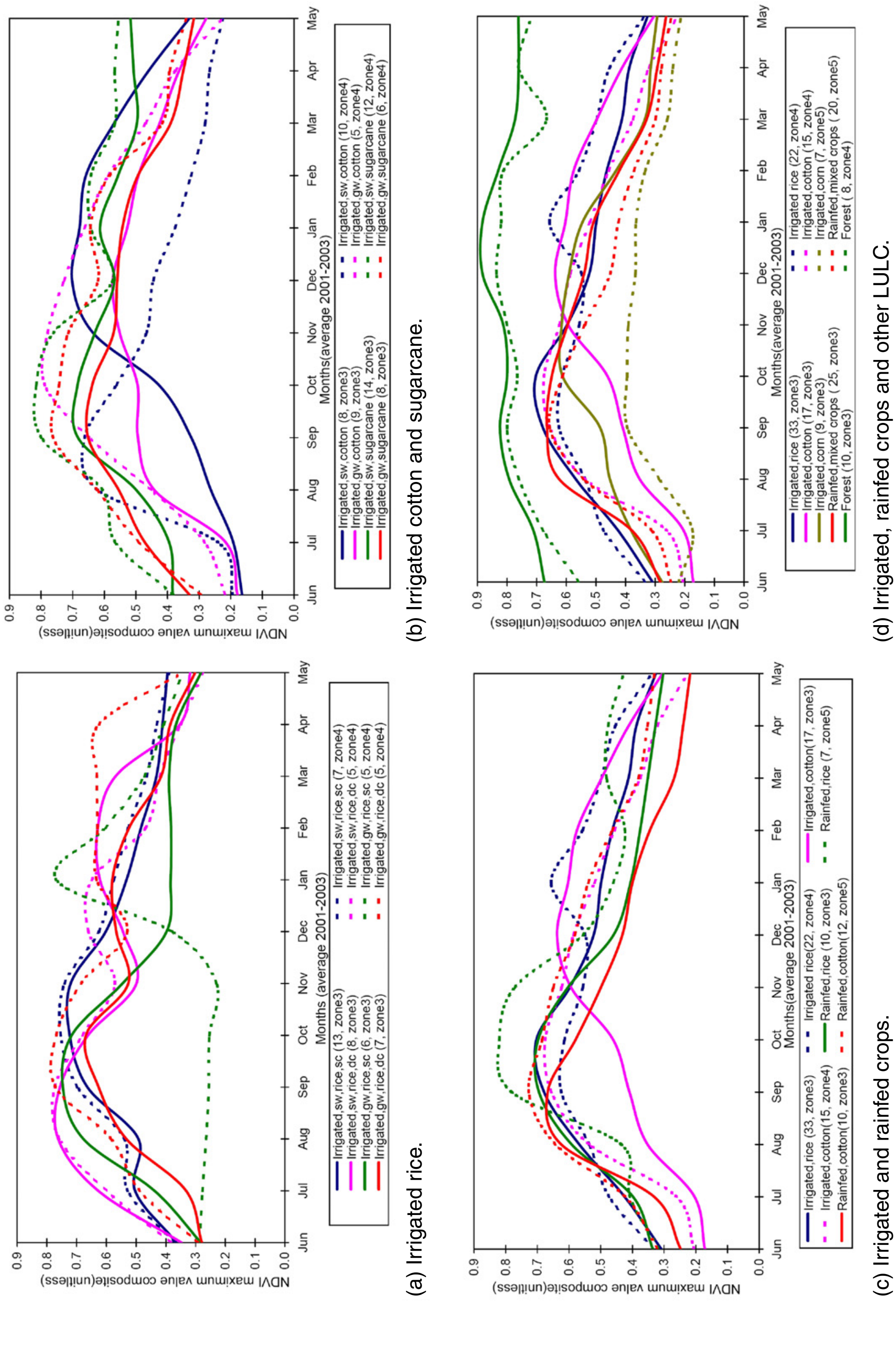

Fig. 6. The ideal spectral data bank illustrated for (a) irrigated rice, (b) irrigated cotton and sugarcane, (c) irrigated and rain-fed areas, and (d) irrigated and other LULC areas. (Note: sample sizes within the brackets of legends).

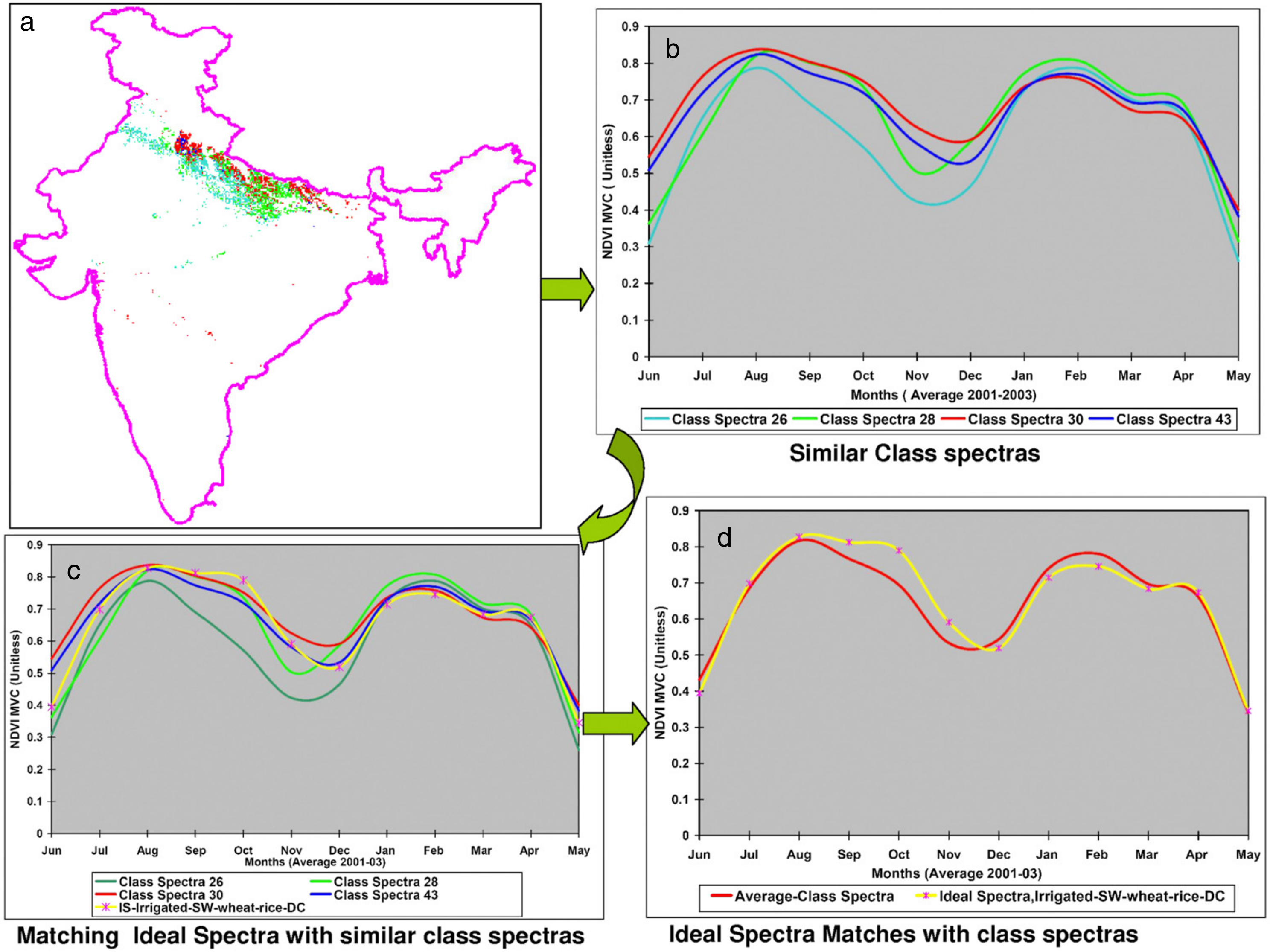

Fig. 7. Spectral Matching Technique (SMTs): Matching class spectra with ideal or target spectra to group and identify classes. The top left figure shows the spatial distribution of the four classes. The top right figure shows the class spectra of these four classes based on unsupervised classes (shown as monthly NDVI averages based on 2001–2003 MODIS 500 m data). The bottom left figure shows the four class spectral signatures with their best match ideal spectral signature (shown in yellow). The bottom right figure shows the ideal spectral signature (yellow) with the average of the four highly correlated class spectra (shown in red).

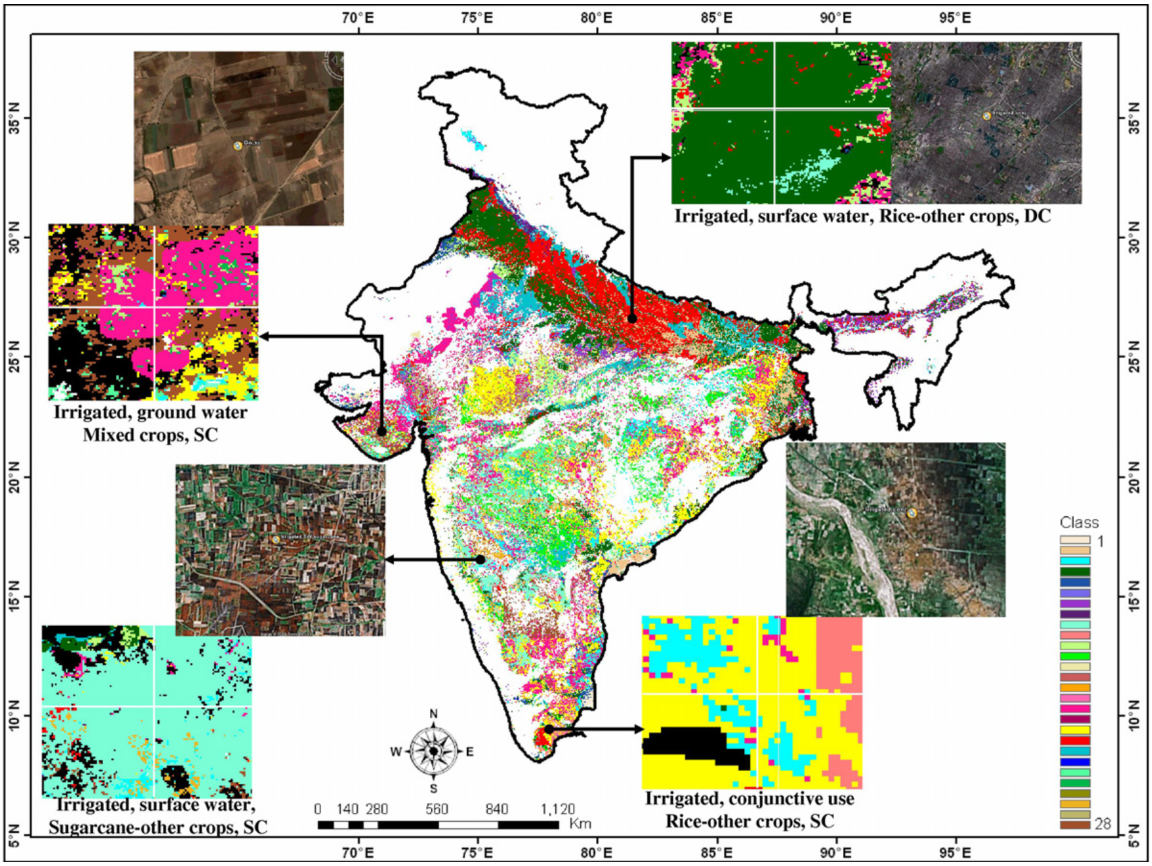

Fig. 8. Class identification and labeling using Google Earth very high resolution imagery.

with similar spectra will have high SCS R^2 values. After grouping, classes 26, 28, 30 and 43 (e.g., Fig. 7) were matched with ISDB and given preliminary labeling as "irrigated-surface water-wheat-rice-double crop".

3.5.2. Class identification and labeling protocol

The classes were identified and labeled according to the following protocol: SMTs as described extensively by Thenkabail et al. (2007a), bispectral plots (Thenkabail et al., 2005) of classes, use of extensive field-plot data (Section 3.3), Google Earth Very High Resolution Imagery (GE VHRI; e.g., Fig. 8), use of secondary data and rule-based decision trees.

The process of SMTs is illustrated in Fig. 7 and described in detail by Thenkabail et al. (2007a). Bispectral plots depict class characteristics by representing the classes in brightness-greenness-wetness in a 2-D feature space (2-d FS) (Kauth and Thomas, 1976; Crist and Cicone, 1984) and are particularly useful in identifying agricultural crops. The application of 2-D FS bispectral plots for identifying irrigated, rain-fed and other LULC classes is illustrated and explained by Thenkabail et al. (2005, 2006). If more than one type of field-plot data points (e.g. irrigated and rain-fed) fall on one class, then that class is considered "mixed" and is selected for further analysis to resolve the class type. Techniques used for further analyses are spatial modeling, decision tree algorithms, and masking and reclassifying (see Fig. 3). Spatial modeling involved taking a mixed class and performing GIS spatial modeling using secondary data such as slope, elevation, evapotranspiration and rainfall, and techniques such as overlay, matrix, recode, sieve and proximity analyses (Lieca, 2007) based on the theory of map algebra and Boolean logic (Tomlinson, 2003). The secondary data are resampled and harmonized to have the same spatial resolution as MODIS data. We explain here the process of resolving a mixed class labeled "croplands mixed with natural vegetation" (taken as an example). Our goal was to separate "croplands" from "natural vegetation". For this we used elevation data and "overlaid" (in a GIS spatial modeling framework such as in ERDAS spatial modeler) the mixed class of "croplands mixed with natural vegetation" with elevation. This separated all natural vegetation that was at a higher elevation from croplands that were at a lower elevation. We further "split" irrigated croplands from rain-fed croplands using evapotranspiration (ET) data. Irrigation existed in areas where ET was significantly less than precipitation. The process can go on until we are able to split a mixed class into two or more distinct classes accurately. Note that one could use multiple secondary layers at once to resolve mixed classes. For example, croplands may exist at a higher elevation, but at a lower slope. In such a case, we use elevation layer along with the slope layer to resolve the mixed class. A rule-based decision tree algorithm was also used to help split the mixed classes (DeFries et al., 1998). The basic process of decision trees involved repeated division of a class through hierarchically structured rules produced from a knowledge base created from training data such as an ISDB or on field knowledge. These rules can be applied to an entire image to produce accurate land cover maps and inventories. One example application is in using NDVI variations in specific months in different parts of the same class to separate the classes. Detailed decision tree rule-based classification approaches are illustrated in our recent work (Biradar et al., 2009; Thenkabail et al., 2009a,b). The mixed classes were masked out and the MFDC covering the mixed class area was used to reclassify (using unsupervised classification) the image into a number of classes that are successfully identified and labeled. This was followed by a repetition of the entire class identification and labeling process. Difficulties were encountered when separating classes with subtle variations in class signatures such as minor irrigation and supplemental irrigation from rain-fed irrigation. In addition to the aforementioned class identification protocols, various approaches were

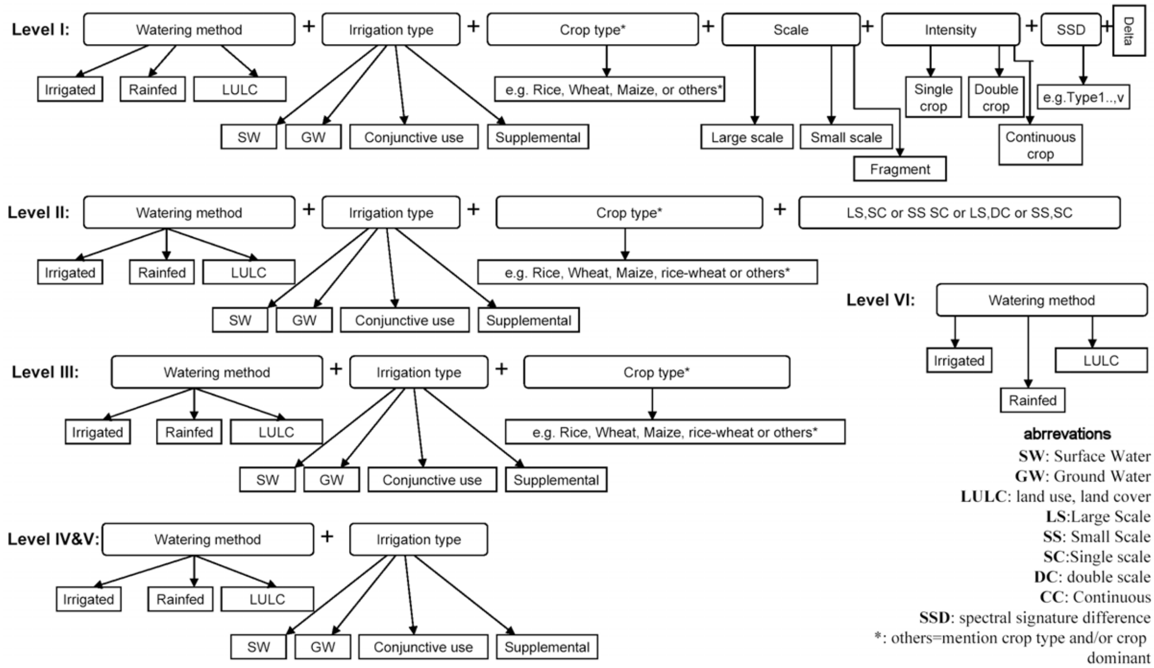

Fig. 9. Standardized class naming convention that follows a hierarchical approach.

used to achieve separation of informal irrigation from rain-fed irrigation and included (a) the use of cropping calendars (irrigated and rain-fed follow unique crop calendars throughout India) detected using NDVI time series; (b) identification of cropping patterns (rain-fed crops are mixed with similar crops in a given area whereas irrigated crops tend to have significantly larger patches); and (c) extensive field-plot data knowledge (Fig. 2). A standardized hierarchical class-naming convention (Fig. 9; Klijn and Udo de Haes, 2004) was adopted. These classes enable obtaining classes at different levels and can be "cross walked" (Torbick et al., 2006). The "cross walk" procedure shows how the classes are aggregated or disaggregated. This way an aggregated class can be tracked to determine which disaggregated classes were combined to form it or vice versa. Whenever over 90% of field-plot data points fall within a given class then that particular class is assigned a class name, and is later further reaffirmed using Google Earth very high resolution imagery (Fig. 8). All classes were named using a standard class naming protocol (Fig. 9). When multiple analysts provide class names, the standardized class naming protocol is very useful.

3.6. Sub-Pixel Area (SPA) calculations

The class areas obtained from the MODIS data provide only the FPAs. The actual areas can be obtained only by computing SPAs (Thenkabail et al., 2007b, 2009a; Biradar et al., 2009), which are defined as:

$$\mathrm{SPA}_n = \mathrm{FPA}_n \times \mathrm{IAF}_n \tag{1}$$

where SPA_n is the sub-pixel area of class n, FPA_n is the full-pixel area of class n and IAF_n is the irrigated area fraction of class n.

The SPA of each class is computed by multiplying the FPA of that class with IAF of the class. Later, the SPAs of all classes are summed to obtain actual area of irrigation from all the classes. The IAF is determined using field-plot data and high-resolution imagery.

The uncertainties and errors in area estimates were reduced to a minimum by using three distinct methods of IAF calculations as described in (Thenkabail et al., 2007b). These IAF calculation methods were (a) Google Earth Estimate (IAF-GEE), (b) high-resolution imagery (IAF-HRI), and (c) sub-pixel decomposition technique (IAF-SPDT). A comprehensive discussion and assessment of these methods by Thenkabail et al. (2007b) showed that the differences in areas calculated by different methods varied by 2%–5%. The robustness of the area calculation was improved by averaging the IAFs of the three methods.

4. Results and discussions

4.1. Irrigated area maps

The study resulted in producing irrigated area maps and statistics. The classes from different segments were combined to produce two irrigated area maps for the study area: a disaggregated irrigated area map with 28 classes (Fig. 10), and an aggregated irrigated area map with only two classes (Fig. 11). Class names in the 28-class map (Fig. 10) consist of irrigation source (surface water, conjunctive use and groundwater), irrigation intensity (single crop, double crop and continuous crop), and crop type. In Fig. 11, all classes were aggregated to either (a) major and medium irrigation by surface water, or (b) minor irrigation by groundwater, small reservoirs, and tanks, showing the widespread use of groundwater in India, which is a result of a swift increase in tube wells from a meager 100,000 in the early 1960s to anywhere between 19 to 26 million by year 2000 (Endersbee, 2005).

The major and medium irrigated command area boundaries (Fig. 4(b)) are provided by the CBIP. According to CBIP, this area is almost exclusively irrigated by surface water reservoirs. This boundary was used to mask the MODIS MFDC, classify it, and identify classes within it using the methods and protocols described in Section 3 and its subsections. The results (Fig. 12) showed that only about 48% of this area is actually irrigated by surface water, nearly 38% by groundwater/conjunctive use, 3% rain-fed and 12% other LULC such as water bodies, forests, barren lands and rangelands.

4.2. Irrigated areas considering and without considering intensity

Two types of irrigated areas were reported: (a) without considering intensity of cropping, referred to as TAAI; and (b) by

Table 1
Irrigated area classes and their areas for India. The disaggregated 28-class sub-pixel irrigated areas (SPIAs) are computed by multiplying full pixel areas (FPAs) with irrigated area factions (IAFs). The areas are reported: (a) without considering intensity (total area available for irrigation (TAAI) or net areas), and (b) considering intensity (annualized irrigated areas or gross areas).

Class #	Class name	FPA Hectares	IAF-TAAI unitless	TAAI Hectares	IAF-Season 1 unitless	AOS1 Hectares	IAF-Season 2 unitless	AOS2 Hectares	IAF-Cont. unitless	AOC Hectares	AIA Hectares
A. Major Irrigation											
1	Irrigated, sw, rice, sc	757,230	0.74	560,350		0	0.74	561,311			561,311
2	Irrigated, sw, rice, dc	5,442,306	0.86	4,680,383	0.86	4,689,907	0.64	3,480,363			8,170,270
3	Irrigated, sw, rice-other crops, sc	7,058,020	0.71	5,011,194	0.71	4,992,079					4,992,079
4	Irrigated, sw, rice-other crops, dc	20,053,220	0.76	15,240,447	0.76	15,308,587	0.60	12,098,424			27,407,011
5	Irrigated, sw, rice-other crops, cc	2,116,728	0.78	1,651,048					0.52	1,107,612	1,107,612
6	Irrigated, sw, wheat-other crops, sc	92,153	0.61	56,213	0.61	55,762					55,762
7	Irrigated, sw, wheat-other crops, dc	5,030,827	0.59	2,968,188	0.59	2,954,353	0.41	2,055,350			5,009,703
8	Irrigated, sw, wheat-other crops, cc	1,000,524	0.74	740,388					0.87	869,706	869,706
9	Irrigated, sw, sugarcane-other crops, sc	8,787,160	0.74	6,502,498			0.65	5,690,927			5,690,927
10	Irrigated, sw, mixed crop, sc	2,158,887	0.68	1,468,043			0.68	1,473,440			1,473,440
11	Irrigated, sw, mixed crops, dc	5,334,504	0.72	3,840,843	0.48	2,559,890	0.57	3,027,051			5,586,941
B.	Minor Irrigation (GW,SR,Tanks)										
12	Irrigated, gw, rice-othercrops, sc	7,673,661	0.63	4,834,407	0.63	4,831,209					4,831,209
13	Irrigated, gw, cotton-other crops, sc	965,814	0.59	569,830	0.55	526,851					526,851
14	Irrigated, gw, cotton, wheat-other crops, dc	2,860,241	0.64	1,830,554	0.59	1,683,606	0.51	1,452,480			3,136,087
15	Irrigated, gw, cotton, soyabean-other crops, cc	11,806	0.83	9,799					0.65	7,643	7,643
16	Irrigated, gw, sugarcane-other crops, sc	651,553	0.73	475,634	0.70	454,157					454,157
17	Irrigated, gw,mixed crops, sc	21,034,124	0.60	12,620,475	0.60	12,629,239					12,629,239
18	Irrigated, gw,plantations-other crops,cc	221,227	0.69	152,647					0.69	152,292	152,292
19	Irrigated, cu, rice-other crops, sc	20,306,539	0.70	14,214,577	0.68	13,842,291					13,842,291
20	Irrigated, cu, rice, wheat-other crops, dc	19,668,895	0.76	14,948,360	0.67	13,274,865	0.57	11,176,850			24,451,715
21	Irrigated, cu, wheat, rice-other crops, dc	11,682,240	0.78	9,112,147	0.65	7,537,251	0.59	6,835,130			14,372,381
22	Irrigated, cu, rice, sugarcane-other crops, cc	63,432	0.77	48,842					0.77	48,922	48,922
23	Irrigated, cu, wheat-other crops, sc	4,011,670	0.70	2,808,169	0.70	2,815,821					2,815,821
24	Irrigated, cu, cotton-other crops, sc	2,287,510	0.64	1,464,006	0.61	1,400,848					1,400,848
25	Irrigated, cu, cotton, wheat-other crops, dc	51,819	0.79	40,937	0.59	30,411	0.71	36,639			67,050
26	Irrigated, cu, sugarcane-other crops, sc	3,008,377	0.74	2,226,199	0.66	1,971,463					1,971,463
27	Irrigated, cu, soyabean, wheat-other crops, dc	1,576,110	0.63	992,949	0.60	953,538	0.39	610,769			1,564,306
28	Irrigated, cu, mixed crops, sc	6,219,928	0.64	3,980,754	0.64	3,974,008					3,974,008
		160,126,505		113,049,883		96,486,136		48,498,733		2,186,175	147,171,043

Note: FPA = full pixel area; IAF-TAAI = Irrigated area fraction for Total area available for irrigation; TAAI = Total area availabel for irrigation; IAF-Season 1 = Irrigated area fraction for Season 1; AOS1 = Area of Season 1; IAF-Season 2 = Irrigated area fraction for Season 2; AOS2 = Area of Season 2; IAF-Continious = Irrigated area fraction for Continuous; AOC = area of Continuous Cropping in a year; AIA = Annualized Irrigated area; SW = Surface water; GW = groundwater ; CU = Conjunctive use; SC = Single Crop; DC = Double Crop; CC = Continuous Crop; SR = Small reservoirs.

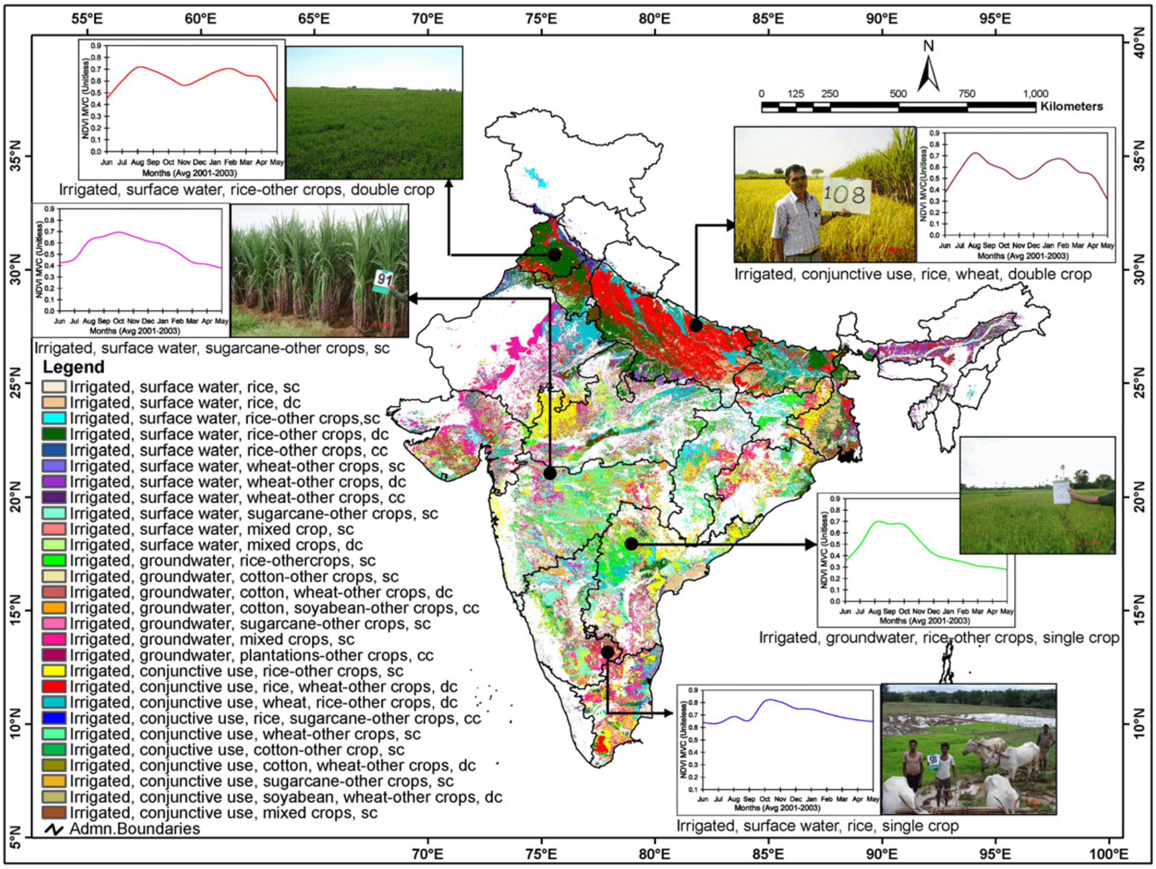

Fig. 10. The final 28 disaggregated irrigated area classes of India based on MODIS data.

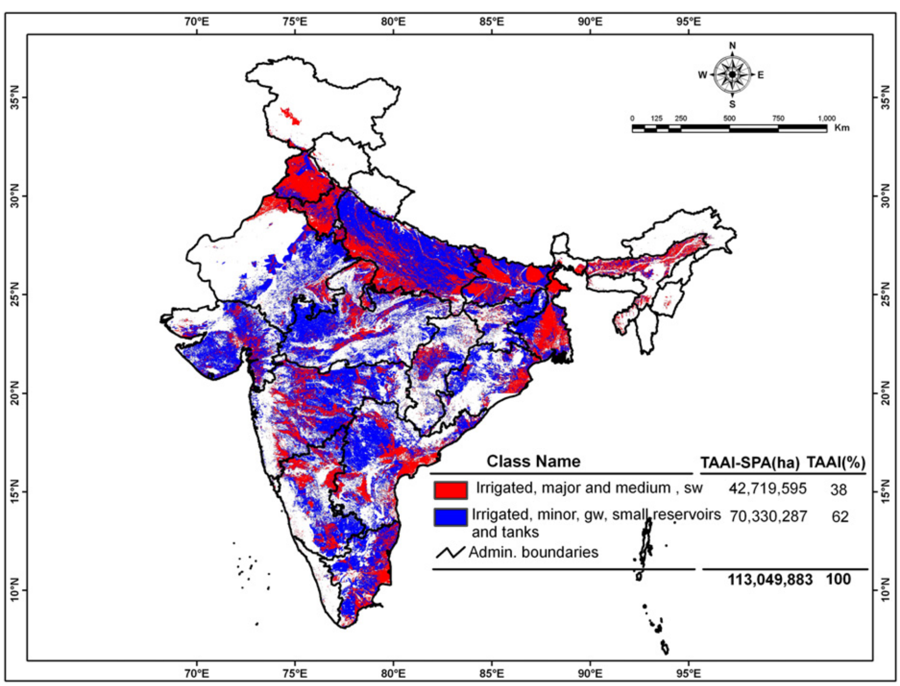

Fig. 11. The two final aggregated irrigated area classes of India based on MODIS time series for 2001–2003.

considering areas of intensified cropping through multiple irrigated areas, referred to as AIAs. Both TAAI and AIA are reported as SPAs, which represent the actual areas. The TAAI and AIA statistics were reported for the 28-class map (Table 1) and for the Indian states (Table 2). The TAAI (Tables 1 and 2) was derived directly from the 28-class irrigated area map (Fig. 10) by multiplying the FPAs of the classes with IAFs. The AIAs (Tables 1 and 2) were determined by multiplying the FPAs with IAFs for each season.

The MODIS-derived TAAI and AIA of India were 113 and 147 MHa, respectively (Table 1). Irrigated rice-dominant double cropping (class 4) was the most prominent class under surface water irrigation (Fig. 10). For the minor irrigation sources, the

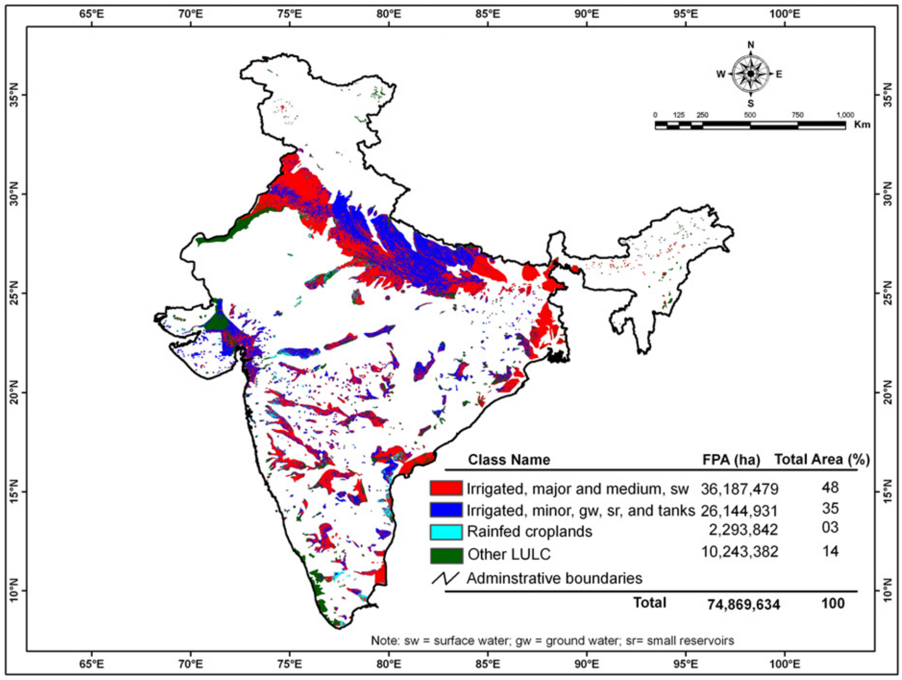

Fig. 12. Aggregated irrigated area classes within India's Central Board of Irrigation and Power boundaries mapped using MODIS time series for 2001–2003.

Table 2
Irrigated areas of India by state. State-by-state irrigated areas of India reported (a) without considering intensity (TAAI or net areas), and (b) considering intensity (annualized irrigated areas or gross areas).

SL (No)	State (Name)	TAAI	SPA-HRI and SPDT (mean): IWMI GIAM-500 m (actual irrigated area)			
		HRI and GEE (mean)	Season 1 (ha)	Season 2 (ha)	Continuous (ha)	Annualized sum (ha)
1	Andaman & Nicobar	0	0	0	0	0
2	Andhra Pradesh	11,655,001	9,452,478	3,735,389	189,903	13,377,771
3	Arunachal Pradesh	94,216	87,199	62,598	1,434	151,230
4	Assam	2,531,447	2,410,390	1,687,035	5,665	4,103,090
5	Bihar	6,171,853	5,817,162	3,859,185	3,953	9,680,300
6	Chattisgarh	3,517,493	3,328,128	268,227	5,528	3,601,883
7	Chandigarh	6,026	4,394	3,404	1,474	9,272
8	Dadra and Nagar Haveli	16,043	13,659	3,232	0	16,891
9	Daman and Diu	41,741	40,292	4,662	0	44,954
10	Delhi	39,928	35,574	24,576	329	60,479
12	Goa	23,272	14,099	14,595	176	28,870
13	Gujarat	6,943,207	6,135,429	1,583,449	139,008	7,857,886
14	Haryana	3,041,243	2,556,291	2,177,755	224,982	4,959,027
14	Himachal Pradesh	89,558	31,775	26,501	62,087	120,364
15	Jammu and Kashmir	395,042	285,753	83,425	115,828	485,007
16	Jharkhand	2,590,682	2,492,336	188,713	146	2,681,195
17	Karnataka	7,259,681	5,312,445	2,297,709	53,248	7,663,401
18	Kerala	113,357	90,451	44,124	17,386	151,961
19	Lakshadweep	0	0	0	0	0
20	Madhya Pradesh	11,623,751	10,308,726	4,963,616	117,696	15,390,039
21	Maharashtra	12,763,374	9,279,588	3,666,826	73,712	13,020,126
22	Manipur	42,245	35,617	11,150	4,220	50,986
23	Meghalaya	66,867	63,178	42,114	648	105,939
24	Mizoram	794	633	606	0	1,238
25	Nagaland	12,126	12,033	8,928	19	20,980
26	Orissa	4,311,877	3,923,981	1,013,158	6,320	4,943,459
27	Pondicherry	32,903	12,333	18,942	5,419	36,694
28	Punjab	3,753,295	3,353,088	2,713,504	308,380	6,374,972
29	Rajasthan	7,789,158	6,634,087	3,426,588	330,356	10,391,032
30	Sikkim	0	0	0	0	0
31	Tamil Nadu	6,317,773	4,784,174	1,568,068	385,749	6,737,992
32	Tripura	144,343	139,432	102,325	90	241,848
33	Uttar Pradesh	16,310,986	14,745,330	11,940,359	93,817	26,779,506
34	Uttaranchal	236,679	189,367	160,031	25,388	374,786
35	West Bengal	4,905,306	4,712,636	2,658,311	10,525	7,381,471
	Total	112,841,267	96,302,057	48,359,104	2,183,484	146,844,646

Note: TAAI: Tota Area available for Irrigation.
SPA: Sub pixel area; HRI: High resolution Image; GEE: Google earth estimation.

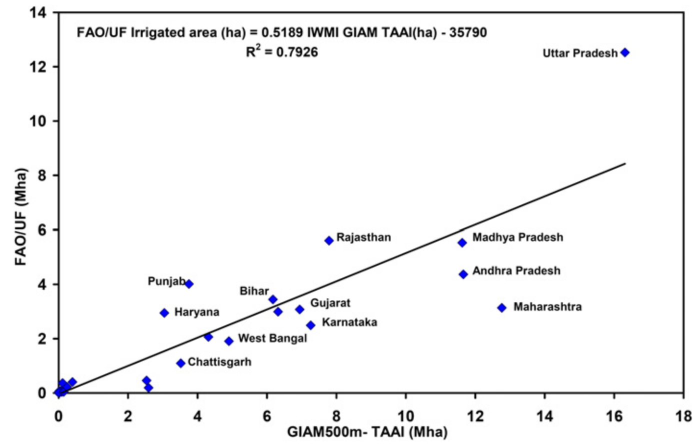

Fig. 13. Comparison of TAAI with FAO/UF. The TAAI is compared with areas equipped for irrigation by FAO/UF.

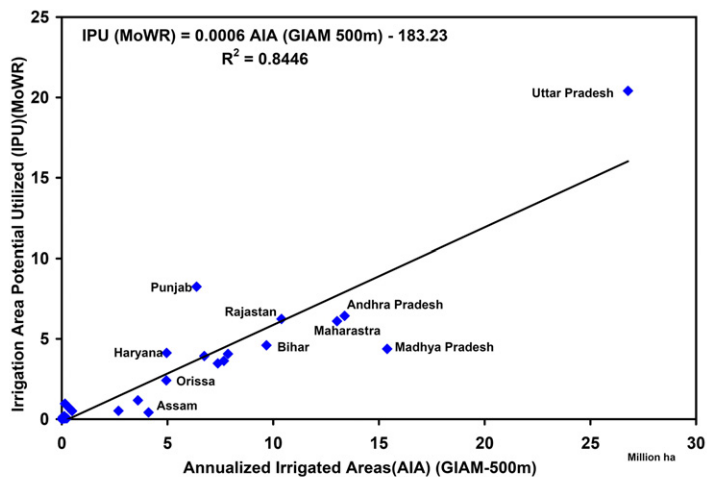

Fig. 14. Comparison of AIA with MoWR data. The annually averaged irrigated area (AIA) is compared with MoWR (MoWR, 2005) and Central Water Commission (CWC) data.

most prominent class was the mixed single crop (class 17), closely followed by rice-dominant single crop (class 19) and rice-wheat-dominant double crop (class 20). Overall, the dominant crops are rice, wheat and cotton (Table 1). State-by-state TAAI and AIA were also computed (Table 2) and were very useful in comparing the statistics for these administrative units obtained from MoWR (2005), FAO/UF (Siebert et al., 2006) and other studies (Thenkabail et al., 2009b).

4.3. Comparisons, accuracies, errors and uncertainties in irrigated areas

The final irrigated areas derived in this study were tested for accuracies, errors and uncertainties based on the field-plot data. Comparisons were made between the MODIS-derived TAAI and an equivalent parameter (areas equipped for irrigation) in the FAO/UF (Siebert et al., 2006) yielding an R^2 value of 0.79 (Fig. 13). The TAAI areas were consistently higher for an overwhelming proportion of the Indian states. The AIAs were related to an equivalent parameter (irrigation potential utilized or IPU) derived by MoWR (2005) yielding an R^2 value of 0.84 (Fig. 14). The MODIS 500 m-derived TAAI and AIA were also compared with the equivalent areas derived using fused AVHRR 10 km and SPOT Vegetation 1 km data reported in (Thenkabail et al., 2009a) providing an R^2 value of 0.97 (Figs. 15 and 16). This match between the two scales indicated consistency of irrigated area estimates using remote-sensing approaches. This is not that surprising given the use of similar methods. However, the areas are larger at finer spatial resolution due to better distinction of fragmented irrigated patches (Velpuri et al., in press) specifically in India where minor irrigation from small tanks and groundwater is widespread (Thenkabail et al., 2006). Ozdogan and Woodcock (2006) reported large errors in area estimates for classes which are possible even when based on accurate thematic maps, and the magnitude of the problems depended on the sub-pixel proportions used to define class memberships and the proportion of the class in the overall study.

Determining accuracy based on Google Earth Very High Resolution Imagery (GE VHRI) provided an overall accuracy of the irrigated areas of 83%, with a 17% error of omission and a 23% error of commission (Table 3). Determining accuracy based on other field-plot data showed an overall accuracy of 89%, with an 11% error of omission and a 33% error of commission (Table 3). Accuracy determined by pooling the Google Earth and other field-plot data showed an accuracy of determining irrigated areas of 88%, with a 12% error of omission and a 32% error of commission suggesting an uncertainty of 20% in determining exact irrigated areas. The errors of commission and omission were mainly due to mixing between the rain-fed and irrigated areas. Some mix between the rain-fed and irrigated classes cannot be avoided at MODIS 500 m resolution (1 pixel = 25 ha) due to the sub-pixel nature of the areas where there are more than one land cover type within a pixel. Areas may be adjusted based on confusion matrices (Card, 1982; Hay, 1979) which are likely to improve our area estimates, but this will require more careful field verification. Resolution is not the only cause of

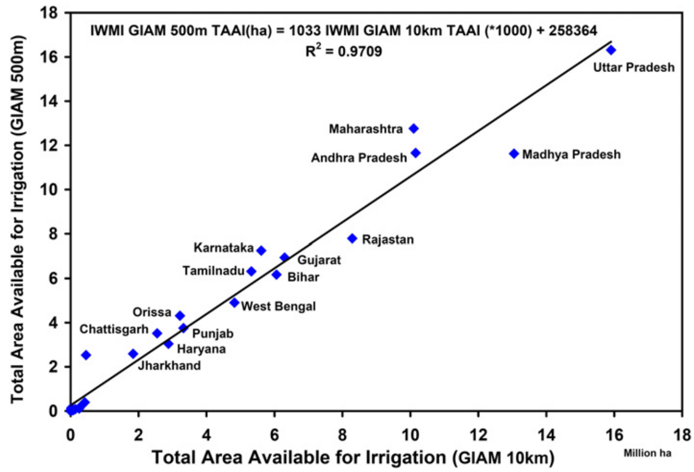

Fig. 15. Comparison of 500 m TAAI with TAAI generated at 10 km. The TAAI computed for the Indian states in this study using 500 m MODIS data is compared with TAAI obtained from 10 km AVHRR data reported in literature (Thenkabail et al., 2009a,b).

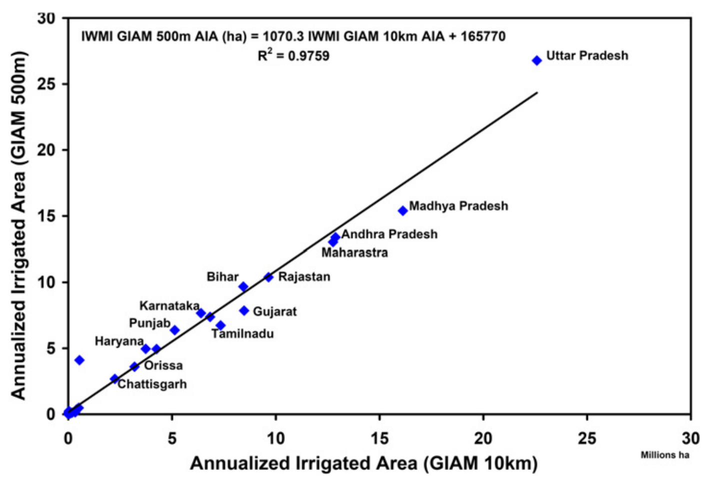

Fig. 16. Comparison of 500 m AIA with AIA generated at 10 km. The AIA computed for the Indian states in this study using 500 m MODIS data is compared with AIA obtained from 10 km AVHRR data reported in literature (Thenkabail et al., 2009a,b).

Table 3
Accuracies and errors. Accuracies and errors were assessed for the irrigated areas using (a) Google Earth imagery, (b) field-plot data, and (c) pooled data from 1 and 2.

Level of accuracy assessment	Accuracy of irrigated area classes (irrigated GT points falling on irrigated areas) (%)	Errors of Omission (Irrigated GT points falling on non-irrigated) (%)	Errors of Commission (non-irrigated GT points falling on irrigated) (%)
1. India accuracy and errors			
GEGT[a]	83[*]	17	23
IMWI + DCP GT[b]	89[*]	11	33
GE + IWMI + DCP GT[c]	88[*]	12	32

[a] Completely Independent GT Datasets.
[b] Partially independent GT Datasets.
[c] Pooled data from 1 and 2.
[*] Overall Accuracy: Google GT—83%; IWMI + DCP GT—89%; Pooled GT—88%.

uncertainty; a detailed discussion on the causes of uncertainties and approaches to overcome them follows in Section 4.4.

4.4. Causes of uncertainties in irrigated areas

Differences between MODIS-derived irrigated areas and non-remote-sensing-based national statistics can be attributed to (a) inadequate accounting of informal or minor irrigation (groundwater, small reservoir and tanks) in the national statistics; (b) definition issues, (c) IAFs, and (d) resolution of the imagery.

4.4.1. Inadequate accounting of minor irrigation

The irrigated area statistics for India were influenced by 162 major and 221 medium surface water reservoirs reported in the CBIP map (CBIP, 1994, Fig. 4b). However, the MoWR (2005) released minor irrigation (small reservoirs, tanks and groundwater) statistics along with major- and medium-irrigation statistics but these statistics do not adequately account for the massive expansion of groundwater irrigation and small reservoir irrigation over the years (Selvarajan, 2001; Thakkar, 1999). For example, groundwater tube wells in India increased from a meager 100,000 in the early 1960s to about 19 to 26 million (Endersbee, 2005) by the end of the year 2000. The overwhelming proportion of these tube wells are used for irrigation. Yet, there are is only a small amount of data on the areas irrigated by these tube wells which are, at best, rough estimates. for the years 1984–85 to 1993–94 (Thakkar, 1999). Also, often unaccounted in irrigation statistics

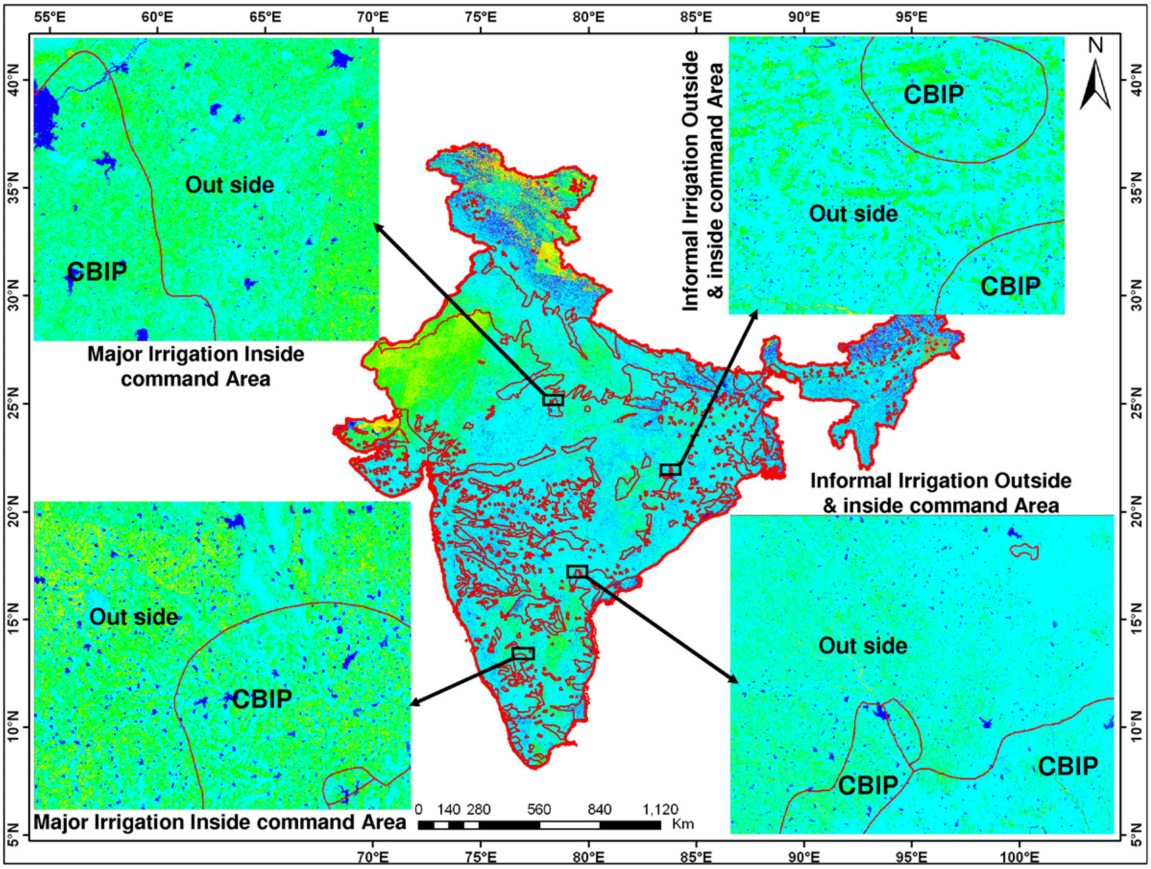

Fig. 17. Surface water (major and minor) irrigated areas within and outside the command areas as shown in a Landsat 30 m mosaic of the study area. The boundaries of the areas irrigated by major and medium surface water reservoirs according to CBIP are shown. The "zoom in views" show surface water reservoirs (major and minor) within and outside CBIP boundaries.

are significant proportions of the small reservoirs and tanks. To highlight these issues, we assembled a fine-resolution Landsat 30 m mosaic of India and highlighted small reservoirs and tanks (Fig. 17). The Landsat non-thermal bands were classified and the water bodies in the classified outputs were identified. This showed a large number of small reservoirs and tanks (see blue areas in Fig. 17). In the Krishna river basin, encompassing about 8% of the study area, 6100 small tanks and small reservoirs (water surface area between 5 ha and 2000 ha) were counted by Velpuri et al. (in press) using Landsat data. In the same area, there were 24 major reservoirs with a surface area greater than 2000 ha. Velpuri et al. (in press) reported that minor sources in the basin irrigated 52% of the area but these values are not adequately accounted by any reported statistics. There are an estimated 1.2 million tanks (Mishra, 1993, 1995) in India, most of them built and maintained by local communities. Some of them are used for drinking purposes and others for irrigation. Minor reservoirs built and maintained by the Public Works Department (PWD) are generally used for irrigation in rural areas and for purposes of drinking and utilities in urban areas. Although these reports and statistics account for most of the government projects, few statistics are gathered for use in private initiatives. Indeed, the overwhelming proportions of the tube wells are a result of private initiatives. We overlaid our field-plot groundwater data points on the Landsat 30 m data (Fig. 17) and found that most of these areas are not included in any known maps and statistics.

The proportion of major irrigation, largely from surface water (classes 1 to 11; Fig. 10), was 38% and that in minor irrigation, mainly from groundwater, small reservoirs and tanks (classes 12 to 28), was 62%. The spatial distributions of major and minor irrigated areas are shown in Fig. 11. The current rate of groundwater expansion is 0.72 MHa per annum, which is clearly unsustainable. Already, the groundwater levels are declining rapidly in the states of Gujarat, Haryana, Punjab, Tamil Nadu, Karnataka and Rajasthan.

4.4.2. Definition issues

Another source of uncertainty is due to a large proportion of previously rain-fed areas that are being currently irrigated through informal sources, specifically from groundwater. The total cropland area estimated during this study was 150 MHa (Thenkabail et al., 2009a) comprising 46% of the geographic area of India. This matches well with the generally quoted proportion of 43% in the national statistics. However, the annualized irrigated area reported in this study was 147 MHa (Tables 1 and 3) which is substantially higher than 84 MHa of the irrigation potential utilized (IPU) as reported by (MoWR, 2005). We see that the total cropland areas reported in the national statistics and in this study are about the same. The differences were in irrigated areas. First, the definitions used to map irrigated areas comprised one of the important causes of this difference. In this study, all areas that had significant supplemental irrigation were mapped as irrigated areas and so was informal irrigation from various minor irrigation sources, such as groundwater, tanks and small reservoirs. In many studies (see Agarwal et al., 2003; Loveland et al., 2000) large proportions of the supplemental irrigated areas of India were mapped and/or accounted as rain-fed.

4.4.3. Irrigated Area Fractions (IAFs)

The sub-pixel areas (SPAs) are true irrigated areas and are determined by multiplying FPAs with IAFs. The accuracy of SPAs is dependent on accuracies of IAFs. The IAFs in this study were determined using three distinct methods reported by Thenkabail et al. (2007b) and hence were considered quite robust. Nevertheless, some uncertainties in IAFs due to estimates could not be avoided (Biggs et al., 2006) leading to uncertainties in areas. The uncertainties in irrigated areas due to uncertainties in IAFs can be reduced by determining the IAFs through better field knowledge of the class.

4.4.4. Resolution of imagery

The resolution of imagery can influence the identification of irrigated areas (Ozdogan and Woodcock, 2006; Velpuri et al., in press; Xiao et al., 2006). Some studies (Thenkabail et al., 2007b; Velpuri et al., in press) showed that irrigated areas increased as the resolutions got finer. This was because at finer resolutions the fragmented areas such as those from groundwater, small reservoirs and tank irrigation can be accounted for more accurately. In contrast, the other studies (Ozdogan and Woodcock, 2006) showed that the coarser the spatial resolution the higher the area estimates. This may happen in two situations: (a) when FPAs are accounted as actual areas instead of SPAs; and (b) in contiguous areas such as very large flat beds of homogeneous irrigated areas. In such situations, finer-resolution imagery will differentiate roads and settlements within irrigated areas, whereas coarser resolution imagery may fully miss them. These results indicated that the resolution can be a major factor in uncertainty of irrigated area estimates.

5. Conclusions

The study demonstrated a comprehensive methodology for estimating irrigated areas using MODIS 500 m every 8-day time series of India for years 2001–2003. The methodology consisted of: (a) MFDC composition involving 952 bands; (b) image segmentation based on climate, elevation and temperature; (c) creation of an ISDB on irrigated areas; (d) generation of class spectra; (e) SMTs to group class spectra and match them with ISDB; (f) class identification and labeling protocol involving bispectral plots, field-plot data, and very high resolution imagery (e.g., from Google Earth); (g) approaches such as spatial modeling and decision tree algorithms to resolve mixed classes; and (h) a standardized hierarchical class naming protocol.

Irrigated areas reported without considering the intensity of irrigation were called total area available for irrigation (TAAI) while (b) those considering the intensities of irrigation were called annualized irrigated areas (AIAs). The TAAI for India was 113 MHa and the AIA was 147 MHa. A particular strength of remote sensing was in its ability to establish AIAs (areas irrigated during different seasons over the same area). The irrigated areas were mapped with an overall accuracy of 88% with an error of omission of 12% and an error of commission of 32%. The TAAI, when compared with its nearest equivalent—the net irrigated areas of India's Ministry of Agriculture statistics—showed an R^2 value of 0.79. The AIAs, when compared with their equivalent—the irrigation potential utilized (IPU) from MoWR—showed an R^2 value of 0.84. However, the AIA was consistently higher than the IPU. The study identified five chief causes of uncertainties in irrigated areas: (a) inadequate accounting of informal irrigation (groundwater, small reservoirs and tanks) in traditional statistics; (b) definition issues in both remote sensing and traditional statistics; (c) irrigated area fractions in remote sensing; (d) imagery resolution in remote sensing; and (e) failure to share adequately the data by various Indian states due to vested interests in water resources in traditional statistics.

Acknowledgements

The authors would like to thank Mr. Sarath Gunasinghe and Mr. Ranjith Alankara for supporting data compilation and all the hard work related to the compilation of field-plot data. Secretarial support from Ms. Arosha Ranasinghe and Ms. Samanmali Jayathilake is much appreciated. Encouragement and support received from Prof. Frank Rijisberman, former Director General of IWMI, is much appreciated. Finally the authors would like to thank Mr. Kingsley Kurukulasuriya for the excellent editing of grammar and English. This definitely improved the quality of the paper. The paper is not internally reviewed by the US Geological Survey (USGS). So, the opinions expressed here are those of the authors and not those of the USGS.

References

Agarwal, S., Joshi, P.K, Shukla, Y., Roy, P.S., 2003. SPOT vegetation multi temporal data for classifying vegetation in south central Asia. Current Science 84 (11), 1440–1448.

Azzali, S., Menenti, M., 1989. Irrigation water management in two Italian irrigation districts. In: Proc. Workshop on Earthnet Pilot Project on LANDSAT-TM application, Frascati, Italy, pp. 41–48.

Bartholome, E., Belward, A.S., 2005. GLC2000: A new approach to global land cover mapping from earth observation data. International Journal of Remote Sensing 26 (9), 1959–1977.

Biggs, T.W., Thenkabail, P.S., Krishna, M.G., Scott, C., Parthasaradhi, G.R., Turral, H., 2006. Irrigated area mapping in heterogeneous landscapes with MODIS time-series, field-plot and census data, Krishna basin, India. International Journal of Remote Sensing 27 (19), 4245–4266.

Biradar, C.M., Thenkabail, P.S., Noojipady, P., Yuanjie, L., Dheeravath, V., Velpuri, M., Turral, H., Gumma, M.K., Reddy, O.G.P., Xueliang, L.C., Schull, M.A., Alankara, R.D., Gunasinghe, S., Mohideen, S., Xiao, X., 2009. A global map of rain-fed cropland areas (GMRCA) at the end of last millennium using remote sensing. International Journal of Applied Earth Observation and Geoinformation 11 (2), 114–129.

Brown, J.F., Pervez, S., Maxwell, S., 2009. Mapping irrigated lands across the United States using MODIS satellite imagery. In: Thenkabail, P., Lyon, G.J., Biradar, C.M., Turral, H. (Eds.), Remote Sensing of Global Croplands for Food Security. CRC Press, Taylor and Francis, Boca Raton, London, New York, pp. 178–198.

Card, D.H., 1982. Using known map category marginal frequencies to improve estimates of thematic map accuracy. Photogrammetric Engineering and Remote Sensing 48 (3), 431–439.

Central Board of Irrigation and Power (CBIP),, 1994. Irrigation Atlas of India, vol. II. Govt. Press, New Delhi, India.

Crist, E.P., Cicone, R.C., 1984. A physically-based transformation of the thematic mapper data—The tassled cap. IEEE Transactions on Geoscience and Remote Sensing 22 (3), 256–263.

DeFries, R., Hansen, M., Townsend, J.G.R., Sohlberg, R., 1998. Global land cover classifications at 8 km resolution: The use of training data derived from Landsat imagery in decision tree classifiers. International Journal of Remote Sensing 19 (16), 3141–3168.

Döll, P., Siebert, S., 2002. Global modeling of irrigation water requirements. Water Resources Research 38 (4), 1–10.

Draeger, W.C., 1976. Monitoring irrigated level acreage using Landsat imagery: An application example. US Geological Survey Open-File Report No. 76–630. Sioux Falls, South Dakota, USA. (Duplicated).

Droogers, P., 2002. Global irrigated area mapping: Overview and recommendations. Working Paper 36. International Water Management Institute, Colombo, Sri Lanka, p. 54.

Endersbee, L., 2005. A Voyage of Discovery: A History of Ideas About the Earth, with a New Understanding of the Global Resources of Water and Petroleum, and the Problems of Climate Change. Frankston, Victoria, Australia.

Galford, G.L., Mustard, J.F., Melillo, J., Gendrin, A., Cerri, C.C., Cerri, C.E.P., 2008. Wavelet analysis of MODIS time series to detect expansion and intensification of row-crop agriculture in Brazil. Remote Sensing of Environment 112 (2), 576–587.

Hay, A.M., 1979. Sampling designs to test land-use map accuracy. Photogrammetric Engineering and Remote Sensing 45 (4), 529–533.

Homayouni, S., Roux, M., 2004. Hyperspectral image analysis for material mapping using spectral matching. The International Archives of Photogrammetry, Remote Sensing and Spatial Information Sciences 35, 1682–1750. Part B7.

Huston, D.M., Titus, S.J., 1975. An inventory of irrigated lands within the state of California based on lands and supporting aircraft data. In: Space Sciences Laboratory Series, vol. 16(56). University of California, Berkeley, California, USA.

Justice, C.O., Townshend, J.R.G., Vermonte, E.F., Masuoka, E., Wolfe, R.E., Saleous, N., Roy, D.P., Morisette, J.T., 2003. An overview of MODIS land data processing and product status. Remote Sensing of Environment 83 (1–2), 3–15.

Kauth, R.J., Thomas, G.S., 1976. The Tasseled Cap—A graphic description of the spectral-temporal development of agricultural crops as seen by Landsat. In: Proc. Symposium on Machine Processing of Remotely Sensed Data. Purdue University, West Lafayette, Indiana, United States, 29 June–1 July 1976, pp. 41–50.

Klijn, F., Udo de Haes, H.A., 2004. A hierarchical approach to ecosystems and its implications for ecological land classification. Landscape Ecology 9 (2), 89–104.

Lal, R., 2004. Soil carbon sequestration in India. Climatic Change 65 (3), 277–296.

Lieca,, 2007. Earth Resources Data Analysis System (ERDAS Imagine9.x) Lieca Geosystems, A.G. Heinrich-Wild-Strasse, CH-9435 Heerbrugg, Switzerland.

Lobell, D.B., Asner, G.P., 2004. Cropland distribution from temporal unmixing of MODIS data. Remote Sensing of Environment 93 (3), 412–422.

Loveland, T.R., Reed, B.C., Brown, J.F., Ohlen, D.O., Zhu, J., Yang, L., Merchant, J.W., 2000. Development of a global land cover characteristics database and IGBP Discover from 1 km AVHRR data. International Journal of Remote Sensing 21 (6–7), 1303–1330.

Lu, D., Weng, Q., 2007. A survey of image classification methods and techniques for improving performance. International Journal of Remote Sensing 28 (5), 823–870.

Ministry of Water Resources (MoWR)., 2005. 3rd Census of Minor Irrigation Schemes (2000–01). New Delhi: Ministry of Water Resources, Govt. of India (on CD-ROM and Web portal).

Mishra, A., 1993. Aaj bhi Khaare Hain Talaab. Gandhi Peace Foundation, New Delhi, India, (in Hindi).

Mishra, A., 1995. Rajstaan ki Rajat Bundain. Gandhi Peace Foundation, New Delhi, India, (in Hindi).

Ozdogan, M., Gutman, G., 2008. A new methodology to map irrigated areas using multi-temporal MODIS and ancillary data: An application example in the continental US. Remote Sensing of Environment 112 (9), 3520–3537.

Ozdogan, M., Woodcock, C.E., 2006. Resolution dependent errors in remote sensing of cultivated areas. Remote Sensing of Environment 103 (2), 203–217.

Rao, P.P.N., Mohankumar, N., 1994. Cropland inventory in the command area of Krishnarajasagar project using satellite data. International Journal of Remote Sensing 15 (6), 1295–1305.

Reddy, G.P.O., Dheeravath, V., Thenkabail, P.S., Chandrakantha, G., Biradar, C.M., Noojipady, P., Velpuri, M., Maji, A.K., 2006. Irrigated areas of India based on satellite sensors and national statistics: Issues and way forward from global irrigated area mapping. In: Proc. International Workshop on Global Irrigated Area Mapping, IWMI, Colombo, Sri Lanka, pp. 25–27 September, (on CD-ROM).

Sakamoto, T., Nguyen, N.V., Ohno, H., Ishitsuka, N., Yokozawa, M., 2006. Spatio-temporal distribution of rice phenology and cropping systems in the Mekong delta with special reference to the seasonal water flow of the Mekong and Bassac rivers. Remote Sensing of Environment 100 (1), 1–16.

Sakamoto, T., Yokozawa, M., Shibayama, M., Ishitsuka, N., Ohno, H., 2005. A crop phenology detection method using time-series MODIS data. Remote Sensing of Environment 96 (3–4), 366–374.

Selvarajan, S., 2001. Sustaining India's irrigation infrastructure, Policy Brief 15, National Centre for Agricultural Economics and Policy Research, ICAR, New Delhi, India, p. 7.

Siebert, S., Doll, P., Hoogeveen, J., Global irrigated area map version 2.1. Center for Environmental Systems Research, University of Kassel, Germany, and FAO, Rome, Italy, 2002. http://www.geo.unifrankfurt.de/ipg/ag/dl/forschung/Global_Irrigation_Map/index.html (accessed August 23, 2009).

Siebert, S., Döll, P., Hoogeveen, J., Faurès, J-M., Frenken, K., Feick, S., 2005. Development and validation of the global map of irrigation areas. Hydrology and Earth System Sciences 9 (5), 535–547.

Siebert, S., Hoogeveen, J., Frenken, K., 2006. Irrigation in Africa, Europe, and Latin America. Update of the Digital Global Map of Irrigation Areas to Version 4. Frankfurt Hydrology Paper 05. University of Frankfurt (Main), Germany and FAO, Rome, Italy, p. 135.

Thakkar, H., 1999. Assessment of irrigation in India, Contributing Paper, Draft Working Paper 1, World Commission on Dams, p. 129.

Thenkabail, P.S., Schull, M., Turral, H., 2005. Ganges and Indus river basin land use/land cover (LULC) and irrigated area mapping using continuous streams of MODIS data. Remote Sensing of Environment 95 (3), 317–341.

Thenkabail, P.S., Biradar, C.M., Turral, H., Noojipady, P., Li, Y.J., Vithanage, J., Dheeravath, V., Velpuri, M., Schull, M., Cai, X., Dutta, R., 2006. An irrigated area map of the world (1999) derived from remote sensing. Research Report 105, International Water Management Institute, Colombo, Sri Lanka, p. 74.

Thenkabail, P.S., Gangadhara Rao, P., Biggs, P., Krishna, T., Turral, M., 2007a. Spectral matching techniques to determine historical land use/land cover (LULC) and irrigated areas using time-series AVHRR Pathfinder datasets in the Krishna river basin India. Photogrammetric Engineering and Remote Sensing 73 (9), 1029–1040.

Thenkabail, P.S., Biradar, C.M., Noojipady, P., Cai, X.L., Dheeravath, V., Li, Y.J., Velpuri, M., Gumma, M., Pandey, S., 2007b. Sub-pixel irrigated area calculation methods. Sensors 7 (11), 2519–2538.

Thenkabail, P., Lyon, G.J., Turral, H., Biradar, C.M., 2009a. Remote Sensing of Global Croplands for Food Security. CRC Press, Taylor and Francis group, Boca Raton, London, New York, p. 556 (48 pages in color). Published in June, 2009.

Thenkabail, P.S., Biradar, C.M., Noojipady, P., Dheeravath, V., Li, Y.J., Velpuri, M., Gumma, M., Reddy, G.P.O., Turral, H., Cai, X.L., Vithanage, J., Schull, M., Dutta, R., 2009b. Global irrigated area map (GIAM), derived from remote sensing, for the end of the last millennium. International Journal of Remote Sensing 30 (14), 3679–3733.

Thiruvengadachari, S., 1981. Satellite sensing of irrigation pattern in semiarid areas: An Indian study. Photogrammetric Engineering and Remote Sensing 47 (10), 1493–1499.

Thiruvengadachari, S., 1983. Irrigated agriculture in Cumbum valley in South India: A Landsat study. In: Proc. Seventeenth International Symposium on Remote Sensing of the Environment. Environment Research Institute of Michigan, Ann Arbor, Michigan, USA, pp. 369–397.

Thiruvengadachari, S., Sakthivadivel, R., 1997. Satellite remote sensing techniques to aid irrigation system performance assessment: A case study in India. Research Report 09, International Water Management Institute, Colombo, Sri Lanka, p. 31.

Tomlinson, R., 2003. Thinking About Geographic Information Systems Planning for Managers. ESRI press, p. 283.

Torbick, N., Lusch, D., Qi, J., Moore, N., Olson, J., Ge, J., 2006. Developing land use/land cover parameterization for climate-land modelling in East Africa. International Journal of Remote Sensing 27 (19), 4227–4244.

Tou, J.T., Gonzalez, R.C., 1975. Pattern Recognition Principles. Addison-Wesley Publishing Company, Reading, Massachusetts.

Velpuri, M., Thenkabail, P.S., Gumma, M.K, Biradar, C.M., Dheeravath, V., Noojipady, P., Li, Y.J., 2009. Influence of Resolution or scale in irrigated area mapping and area estimations. Journal of Photogrammetry and Remote Sensing (in press).

Vermote, E.F., El Saleous, N.Z., Justice, C.O., 2002. Atmospheric correction of MODIS data in the visible to middle infrared: First results. Remote Sensing of Environment 83 (1–2), 97–111.

Wall, S.L., 1979. California's irrigated lands. In: Proc. Symposium on Identifying Irrigated Lands Using Remote Sensing Techniques: State of the Art. US Geological Survey EROS Data Center, Sioux, South Dakota, USA, pp. 71–75. 15–16 November 1979.

Wardlow, B.D., Egbert, S.L., 2008. Large-area crop mapping using time-series MODIS 250 m NDVI data: An assessment for the US Central Great Plains. Remote Sensing of Environment 112 (3), 1096–1116.

Wardlow, B.D., Egbert, S.L., Kasten, J.H., 2007. Analysis of time-series MODIS 250 m vegetation index data for crop classification in the US Central Great Plains. Remote Sensing of Environment 108 (3), 290–310.

Xiao, X., Boles, S., Frolking, S., Li, C., Babu, J., Salas, Y., Moore, W., 2006. Mapping paddy rice agriculture in South and Southeast Asia using multi-temporal MODIS images. Remote Sensing of Environment 100 (1), 95–113.